CHALMERS
UNIVERSITY OF TECHNOLOGY

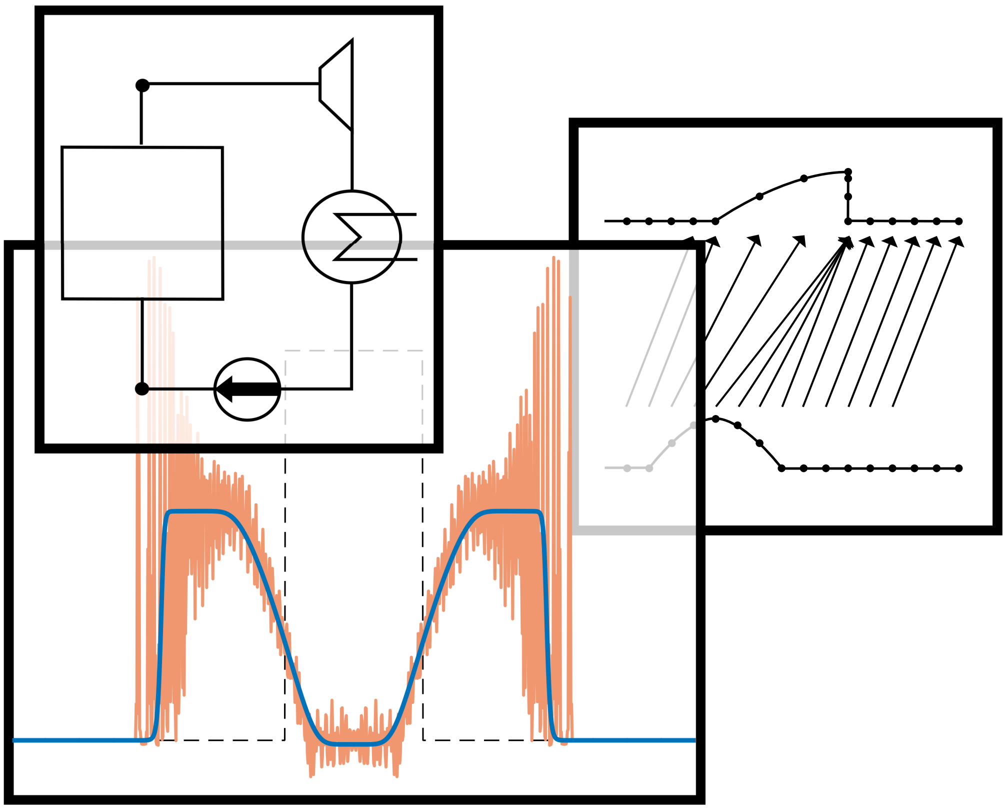

Numerical Analysis of Hyperbolic Multi-Phase Flow Using Entropy Stable Schemes

Master's thesis in Nuclear Science and Technology

MICHAEL JOHANSSON

Department of Physics
CHALMERS UNIVERSITY OF TECHNOLOGY
Gothenburg, 2017
CTH-NT-327

CTH-NT-327

MASTER'S THESIS IN NUCLEAR SCIENCE AND TECHNOLOGY

Numerical analysis of hyperbolic multi-phase flow using entropy stable schemes

MICHAEL JOHANSSON

Examiner: Christophe Demazière

Supervisor: Mikael Fjällborg

Supervisor: Joakim Holmström

CHALMERS
UNIVERSITY OF TECHNOLOGY

Department of Physics
Division of Subatomic and Plasma Physics
CHALMERS UNIVERSITY OF TECHNOLOGY
Gothenburg, Sweden 2017

Numerical analysis of hyperbolic multi-phase flow using entropy stable schemes

Michael Johansson

Examiner:	Christophe Demazière
Supervisor:	Mikael Fjällborg
	Joakim Holmström

Cover Illustration

Top Left:	Basic overview of a nuclear power plant, see Figure 1.1.
Top Right:	Characteristics of a system resulting from a shock wave, see Figure 2.2.
Bottom:	Result comparison between entropy conservative and entropy stable systems, see Figure 4.5.

Master's Thesis 2017
CTH-NT-327
Department of Physics
Division of Subatomic and Plasma Physics
Chalmers University of Technology
SE-412 96 Gothenburg
Telephone +46 31 772 1000

Preface

I would like to take this opportunity to thank the people that made this thesis possible. First my supervisor Mikael Fjällborg who initially suggested this project and the help he and Joakim Holmström has provided. Other significant contributions to this thesis were made by Christope Demazière for taking the role as examiner and Simon Persson as my opponent who both has provided great feedback. I also want to extend my gratitude to both Chalmers Univeristy of Technology for the years I have spent there and Vattenfall for the assistance they provided during this project. Finally I am thankful for the overall support provided by my family and friends.

Michael Johansson, 2017

Abstract

Nuclear power plants generate electricity through the steam power cycle so understanding the behaviour of the fluid is essential. This is done by studying the thermal hydraulics of the system which is governed by several conservation equations. These conservation equations cannot be solved analytically so instead one has to rely on numerical methods and computer codes to simulate the state of the system. In this thesis we look at two-phase systems where discontinuities are present and we see that standard and simple numerical methods such as finite volume schemes are not sufficient and yield unphysical results. Instead we take a different approach by studying entropy and path conditions of the system to create entropy stable path consistent schemes that are able to give a physical solution. We start from a standard two-fluid model and through several approximations we establish a two-phase system that is hyperbolic in nature. The pressure term in the system depends on the fluid and can therefore be expressed in multiple ways and in this thesis we study three ways to express the pressure. The first two ways are based on previously studied one-phase systems where the fluid is either in a pure liquid or gas phase. The last study of the pressure is expressed as an adiabatic process to give a more physical pressure expression which results in a pure two-phase expression that has previously not been studied. We design entropy stable schemes for these systems and test them on two scenarios to show how they react to two realistic discontinuities in the system. The results show that entropy stable schemes are able to handle discontinuities and converge towards a solution where other numerical methods were unsuccessful.

Keywords: Multi-phase flow, CFD, Hyperbolic Systems, Numerical Analysis, ESPC, Entropy Stable Schemes, Shock Wave

Contents

Nomenclature

α	Void fraction
β	Degrees of freedom in gas
η	Entropy function
γ	Adiabatic index
μ	Viscosity
ϕ	Entropy potential
ρ	Density
σ	Shock speed
$\mathbf{v}$	Entropy variables
ξ	Momentum
c	Speed of sound
K	Pressure constant
m	Liquid density ($(1-\alpha)\rho_l$)
n	Vapour density ($\alpha\rho_v$)
P	Pressure
Q	Pressure potential
q	Entropy flux
u	Fluid velocity

Chapter 1

Introduction

We start this chapter by going through how a nuclear power plant generates electricity without going into much detail. Nuclear power is governed by multiple coupled fields of physics but for the scope of this thesis we will mainly be studying thermal hydraulics. Finally we cover some of the tools used in the industry and a more detailed aim of this thesis.

1.1 Nuclear Power Plant Basics

Nuclear power plants essentially operate in the same as manner a coal or natural gas power plant where liquid water is heated turning it into steam. Electrical energy is generated by having the steam pass through a turbine connected to a generator. Before the fluid is heated again it is turned back into liquid phase and cooled using a condenser and heat exchanger. The whole process is commonly referred to as the steam power cycle. The main difference between a nuclear power plant and other heat-based power plants lies in how heat is generated. In a coal or natural gas plant the fuel is burned to produce excess heat with carbon dioxide, sulphur dioxide, and nitrogen oxides among others as byproducts. In a nuclear power plant the heat is generated through the nuclear fission process which does not produce any greenhouse gases but rather radioactive waste. The basic schematic of a nuclear power plant can be seen in Figure 1.1 and note that the connections in this figure and subsequent figures may vary depending on reactor design. The design of the heat source may also quite significantly vary. This section will focus on the two most common commercial reactors which are the Pressurized Water Reactor (PWR) and Boiling Water Reactor (BWR) which both are Light Water Reactors (LWR).

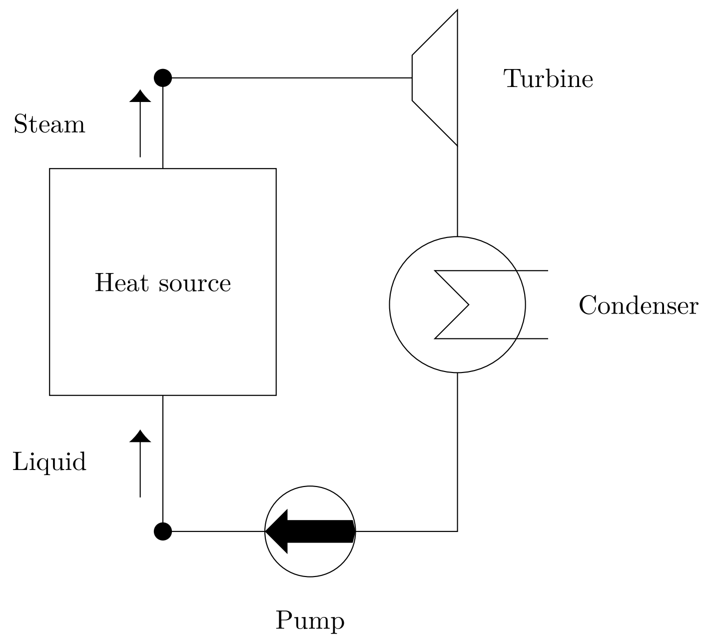

Figure 1.1: *The basic schematic of a nuclear power plant. Cold liquid water enters the heat source through the bottom connection where it becomes dry steam. The steam exits the heat source through the top connection and goes into the turbine generating electricity by taking energy from the steam thus cooling it. The water is further cooled using a condenser turning it into liquid before again entering the heat source through the cold leg. Note that the position of connections may vary depending on the reactor model.*

The schematic of the heat source of a boiling water reactor can be seen in Figure 1.2 and connecting the dots with Figure 1.1 we get the complete reactor. In this reactor design the water often enters the core through the bottom connection which is commonly referred to as the feedwater line. The water is heated in the core and in order to get dry steam to prevent turbine damage we also employ steam separators and steam driers. Once dry steam has been produced it leaves the heat source through the top connection, also known as the steam line.

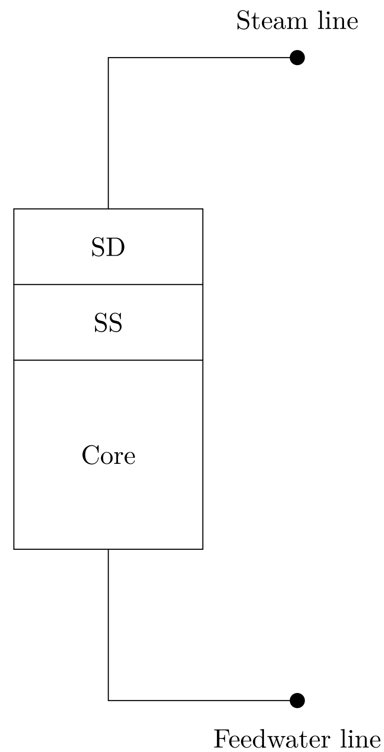

Figure 1.2: *The basic schematic of a BWR. Water enters the core through the bottom connection and is heated. The turbines can be damaged from droplets in the steam so we use steam separators (SS) and steam driers (SD) to produce dry steam.*

Connecting of the heat source of the PWR seen in Figure 1.3 we see that the plant consists of two separate systems. The primary system includes the core and the secondary system connects the heat source to the rest of the plant.Starting with the primary system the pressure inside the system is increased to about 155 bar and using the pressurizer the pressure inside the system can be regulated. The increased pressure results in a higher saturation temperature so the water that is heated in the core does not vapourize and the fluid in the primary system essentially consists of liquid phase water and the heated water then goes into the steam generator. The steam generator acts as a heat exchanger where the generated heat in the primary system is transferred to the secondary system. The secondary system is of lower pressure at approximately 70 bar which means the saturation temperature is lower and the transfer in heat causes the water in the secondary system to boil and leave the steam generator as dry steam.

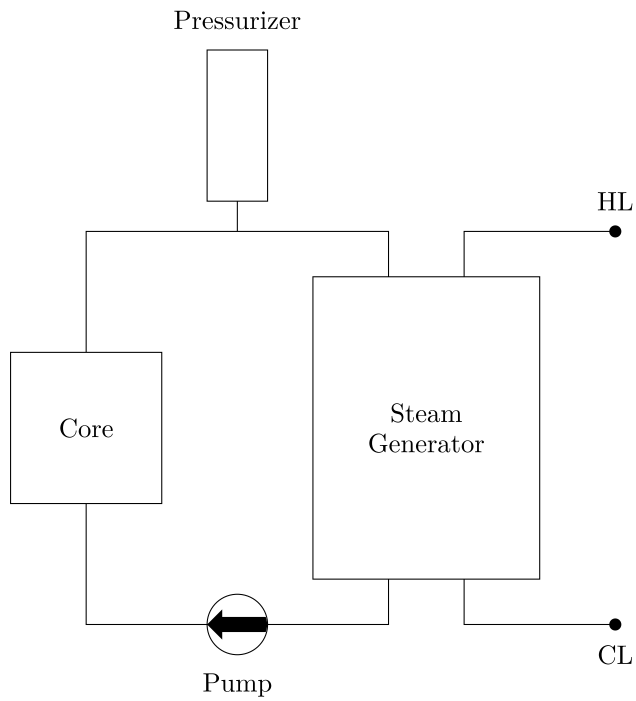

Figure 1.3: *The basic schematic of a PWR. Compared to the BWR this system is separated into two subsystems. The subsystems are known as the primary side which includes the core and the secondary side which connects to the rest of the plant through the cold and hot leg to the plant.*

Besides the difference shown in Figures 1.2 and 1.3 there are other significant differences; especially in the core design which is not covered here. Regardless of these differences we have boiling of liquid water into steam making both types of reactors multi-phase systems.

1.2 Thermal Hydraulics

In nuclear engineering there are mainly two fields of physics used to explain how a nuclear reactor operates. The first is neutron kinetics which is mainly used to calculate the behaviour of neutrons in the core. The second one is called thermal hydraulics and it is the combination of thermodynamics/heat transfer and hydraulics/fluid dynamics. A simple way to explain it is “heated fluid in motion” and is mainly governed by several conservation laws. The first one is the conservation of mass also known as the continuity equation and the second is conservation of momentum which originates in Newton's second law of motion. If the fluid is heated we add conservation of energy but we can also choose between conservation of enthalpy or temperature if more suitable. If we have a multi-phase system and if one uses the so called two-fluid model, we will have a conservation equation for each quantity for each phase with added terms of transfer between the phases. These conservation equations can all be derived from the general transport theorem by using a control mass approach.

The conservation equations that describe the system are differential in nature and can not be solved analytically. Instead we rely on numerical methods and computer codes to simulate the system's behaviour. Computer codes are separated into two categories; System codes work on a macro scale and are used to simulate the entire system. The other type is Computational Fluid Dynamics (CFD) that is often used on a smaller scale to give a more detailed and accurate representation of the flow and thus making CFD more computer intensive. System codes are used to simulate the general behaviour of the reactor while CFD can be used to study sensitive regions such as the core or when higher accuracy is required. The numerical methods used in these codes never give an exact solution and since the methods used vary, different computer codes may lead to different results. Due to the conservative nature of the nuclear industry newly implemented code needs to be rigorously tested and approved which is done by comparing simulated results to experimental data or results from already approved codes.

One computer code used widely in the nuclear industry is TRAC/RELAP Advanced Computational Engine (TRACE) maintained by the U.S Nuclear Regulatory Commission (NRC). TRACE is a one- or three-dimensional code based on the two-fluid model that can be used to either simulate normal or abnormal operating conditions including possible accident scenarios like a Loss of Coolant Accident (LOCA) [1]. Although the NRC is in charge of TRACE development, any of its licensed users is able to make internal modifications to the code and even recommend upgrades. In general TRACE uses first order numerical methods but can be extended to use second order solvers except for the momentum equation which means it is hard to capture fast transients such as water hammers. Discontinuities or high order spatial discretization can cause oscillations in the system and since these oscillations are unphysical a flux limiter is used to control and dampen them. The flux limiter itself however is not a physical response in the system and does not represent how the system prevents oscillations.

1.3 Aim

Sweden is one of the countries participating in NRC's Code Applications and Maintenance Program (CAMP) which is aimed at improving the thermal hydraulic codes maintained by the NRC [2]. The Swedish radiation safety authority known as Strålsäkerhetsmyndigheten (SSM) pays a fee to NRC and in return gets access to the codes for testing possible improvements. As owners and operators of commercial nuclear power plants here in Sweden, SSM has provided these codes to Vattenfall along with the task of possible improvements.

The conservative mindset of the nuclear industry makes improving these codes difficult but there is also a continuous drive for increased safety. Being able to capture fast transients allows users to further improve initial designs or identify weak spots in existing systems. TRACE's inability to capture these forces users to either use other software or simply neglect possible accident conditions. This project is aimed at correcting this deficiency by defining high order numerical solvers for all conservation equations and also using an actual physical response to prevent oscillations rather than using a flux limiter scheme. Project results are continuously checked and verified using previous work in the field and interesting results are compiled into a suggestion of future upgrades to TRACE.

Chapter 2

Background & Theory

This chapter gives an overview of the mathematical theory that we are going to apply to our system. We will begin by looking at hyperbolic equations and why some systems are considered conservative. After that we will go through basic shock theory showing why they happen and how it prevents us from finding a simple solution to the system. As we can not use simple numerical methods we will instead study entropy conditions of the system using a generalization of the methods in [3]. In the last part of this chapter we look at different methods of time discretization and required stability criteria.

2.1 Hyperbolic Systems

From [4] we have that system of one dimensional hyperbolic partial differential equations can be written as

$$\tilde{\mathbf{w}}_t + A(\tilde{\mathbf{w}})\tilde{\mathbf{w}}_x = 0 \tag{2.1}$$

where x and t refer to the time and spatial derivatives, $\tilde{\mathbf{w}}(x,t) : \mathbb{R} \times \mathbb{R}_+ \to \mathbb{R}^n$, and $A(\tilde{\mathbf{w}}) : \mathbb{R}^n \to \mathbb{R}^{n\times n}$ is a square matrix of size $n \times n$ with real and distinct eigenvalues. Hyperbolic systems are characterized by that perturbations of the system does not affect the whole system instantaneously but travel through the system with finite propagation speed. Examples of Hyperbolic systems are multi-phase systems, the Burger's equation, and certain types of transport equations. The models used in modern system codes are not hyperbolic but with the approximations used in this thesis we will see that our system is hyperbolic.

If the matrix A is the Jacobian of some function $\mathbf{f}(\mathbf{w}) : \mathbb{R}^n \to \mathbb{R}^n$, i.e. $A = \nabla_{\mathbf{w}}\mathbf{f}(\mathbf{w})$, the system is considered conservative and Equation (2.1) can be written as

$$\mathbf{w}_t + \mathbf{f}(\mathbf{w})_x = 0. \tag{2.2}$$

using the chain rule. The system is considered conservative since

$$\begin{aligned} \int_a^b \mathbf{w}_t dx + \int_a^b \mathbf{f}(\mathbf{w})_x dx &= 0 \\ \frac{d}{dt}\int_a^b \mathbf{w} dx + \Big[\mathbf{f}(\mathbf{w})\Big]_a^b &= 0 \\ \frac{d}{dt}\int_a^b \mathbf{w} dx + \mathbf{f}(\mathbf{w}(b,t)) - \mathbf{f}(\mathbf{w}(a,t)) &= 0 \end{aligned} \tag{2.3}$$

and $\mathbf{f}$ is the flux of $\mathbf{w}$ meaning that the change in $\mathbf{w}$ over time in the volume between a and b is equal to the transfer at the two interfaces. This means that the quantities in $\mathbf{w}$ are neither being created or destroyed in the volume so $\mathbf{w}$ is a vector of conserved quantities and Equation (2.2) is a system of conservation laws.

If there is formal equivalence between a conservative and a non-conservative system we can transform between them. By multiplying the conservative system in Equation (2.2) by a change-in-variable matrix $T(\mathbf{w}) : \mathbb{R}^n \to \mathbb{R}^{n\times n}$ defined as $T(\mathbf{w}) = \nabla_{\mathbf{w}}\tilde{\mathbf{w}}(\mathbf{w})$ from the left we get

$$\begin{aligned} \nabla_{\mathbf{w}}\tilde{\mathbf{w}}(\mathbf{w})\mathbf{w}_t + \nabla_{\mathbf{w}}\tilde{\mathbf{w}}(\mathbf{w})\mathbf{f}(\mathbf{w})_x &= 0 \\ \tilde{\mathbf{w}}_t + \nabla_{\mathbf{w}}\mathbf{f}(\mathbf{w})\tilde{\mathbf{w}}_x &= 0 \\ \tilde{\mathbf{w}}_t + A(\tilde{\mathbf{w}})\tilde{\mathbf{w}}_x &= 0 \end{aligned} \tag{2.4}$$

which is the non-conservative system in Equation (2.1).

2.2 Shock Theory

In non-linear hyperbolic systems we have formation of shocks as a result of discontinuities and the reason for shock formation can be seen by studying the characteristics of a system [5]. We start by studying a linear hyperbolic equation of the form

$$u_t + au_x = 0. \tag{2.5}$$

By studying this system we find that $u(x(t), t)$ to be a constant for each characteristic and we can see an example of this in Figure 2.1. In this system the characteristics are straight lines with slope a since

$$\frac{dx}{dt} = a \tag{2.6}$$

and the system has well defined solution which is

$$u(x,t) = u(x - at, 0). \tag{2.7}$$

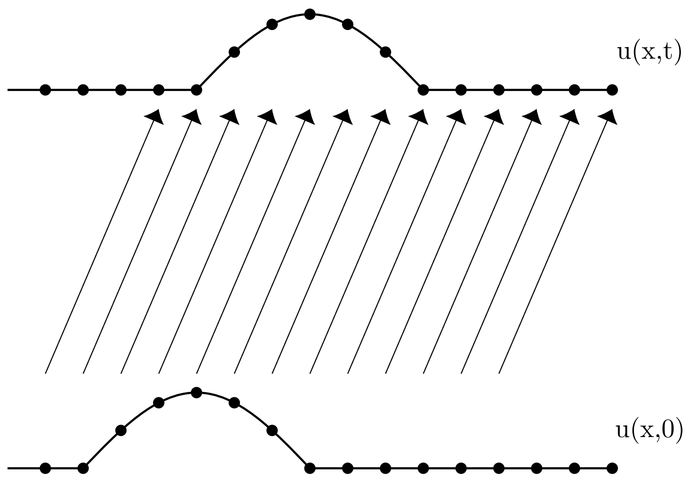

Figure 2.1: *The evolution and characteristics of the system in Equation* (2.5). *Since* $u(x(t), t)$ *is constant for each characteristic the characteristics are all straight lines with constant slope* a.

If we instead study a non-linear system like the Burger's equation

$$u_t + uu_x = 0 \tag{2.8}$$

we still have that the characteristics are still straight lines due to constant $u(x(t), t)$. This time the slope of the characteristics is u which means that the characteristics will no longer be parallel lines and we can see this in Figure 2.2. In the figure we see that as u increases the slope of the characteristics increases which means that several characteristics start approaching the same point. At this point the system still has a unique solution since no two characteristics have the same end-point.

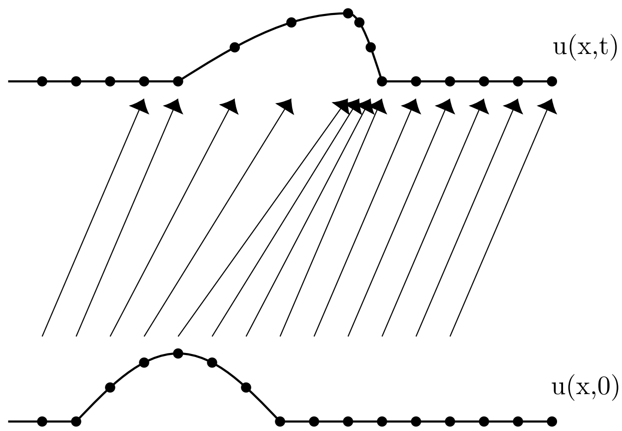

Figure 2.2: *The evolution and characteristics of the system in Equation* (2.8)*. We still have that $u(x(t), t)$ is constant for each characteristic so the characteristics are all straight lines but the slope is no longer constant but rather u. This means that for some x the characteristics become further apart and at other points they come together.*

In the previous figure we saw that even though the characteristics approach a singular point they still are uniquely defined which results in a unique solution. If we study the same system at a later time step we get the results in Figure 2.3 and now we clearly see that several characteristics have all come together to a single point. This results in a discontinuity of u referred to as a shock and u no longer differentiable in the entire system.

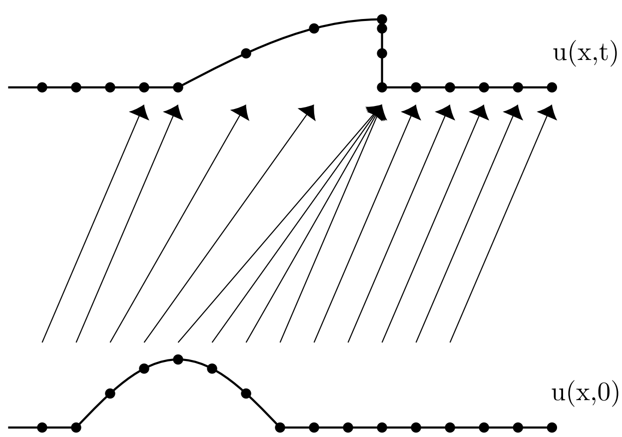

Figure 2.3: *The evolution and characteristics of the system in Equation* (2.8) *but at a later time step than Figure 2.2. The characteristics have now come together and the resulting discontinuity is known as a shock.*

As we saw for the Burger's equation in Equation (2.8) and Figure 2.2 that even though the system starts out with smooth initial data we still have shock formation. The presence of a shock makes u non-differentiable which means the system can not be solved. A way around this is to define a generalized solution, also known as a weak solution, to the system and this can be done for any conserved hyperbolic system defined in Equation (2.2). We start by multiplying the system with a function $\phi(x,t) \in C^1(\mathbb{R}\times\mathbb{R})$ which has compact support and integrate over both time and space resulting in

$$\int_{-\infty}^{\infty}\int_{-\infty}^{\infty} \phi \mathbf{w}_t dt dx + \int_{-\infty}^{\infty}\int_{-\infty}^{\infty} \phi \mathbf{f}(\mathbf{w})_x dt dx = 0. \tag{2.9}$$

Assuming we can change the order of integration we can integrate by parts and get

$$\int_{-\infty}^{\infty} \left(\Big[\phi \mathbf{w}\Big]_{t=-\infty}^{t=\infty} - \int_{-\infty}^{\infty} \phi_t \mathbf{w} dt \right) dx + \int_{-\infty}^{\infty} \left(\Big[\phi \mathbf{w}\Big]_{x=-\infty}^{x=\infty} - \int_{-\infty}^{\infty} \phi_x \mathbf{f}(\mathbf{w}) dx \right) dt = 0 \tag{2.10}$$

and since $\phi(x,t)$ has compact support the first and third term go to zero resulting in

$$\int_{-\infty}^{\infty}\int_{-\infty}^{\infty} \phi_t \mathbf{w} dt dx + \int_{-\infty}^{\infty}\int_{-\infty}^{\infty} \phi_x \mathbf{f}(\mathbf{w}) dx dt = 0. \tag{2.11}$$

Comparing Equations (2.2) and (2.11) we see that they are equivalent if u is differentiable. However if u is not differentiable but still a solution to Equation (2.11) it is said that u is a weak solution to Equation (2.2). The problem with weak solutions is that they are not always unique and in order to get a physical solution further conditions are required [6].

2.3 Numerical Schemes

A popular numerical method for hyperbolic systems is the finite volume scheme. Dividing the system into constant interval of length Δx we get that a numerical solution to the conservative system in Equation (2.2) can be written as

$$\frac{d\mathbf{w}}{dt} + \frac{1}{\Delta x}\left(\mathbf{F}_{i+1/2} - \mathbf{F}_{i-1/2}\right) = 0 \tag{2.12}$$

for some flux function $\mathbf{F}$. The presence of shocks in the system makes the system unsolvable using simple numerical methods since the solution will become susceptible to oscillations and diffusion. To demonstrate this we study the Burger's equation in Equation (2.8) where we have that

$$\mathbf{f}(\mathbf{w}) = \frac{u^2}{2} \tag{2.13}$$

and setting

$$\mathbf{F}_{i+1/2} = \bar{\mathbf{f}} = \frac{\mathbf{f}_{i+1} + \mathbf{f}_i}{2} \tag{2.14}$$

we get

$$\frac{du}{dt} + \frac{1}{2\Delta x}\left(u_{i+1}^2 - u_{i-1}^2\right) = 0. \tag{2.15}$$

The solution to this system with the Heaviside function $\Theta(x)$ as initial condition

$$u(x,0) = 1 + \Theta(x - 0.5) = \begin{cases} 1, & x < 0.5 \\ 2, & x > 0.5 \end{cases} \tag{2.16}$$

can be seen in Figure 2.4. We see that the system starts to oscillate at lower valued point of the discontinuity and eventually the entire system will oscillate. At the upper point of the discontinuity we see that the solution is diffusing trying to even out the system. Different system will have different amounts of oscillations and diffusion but the presence of either makes the system unsolvable using simple numerical methods.

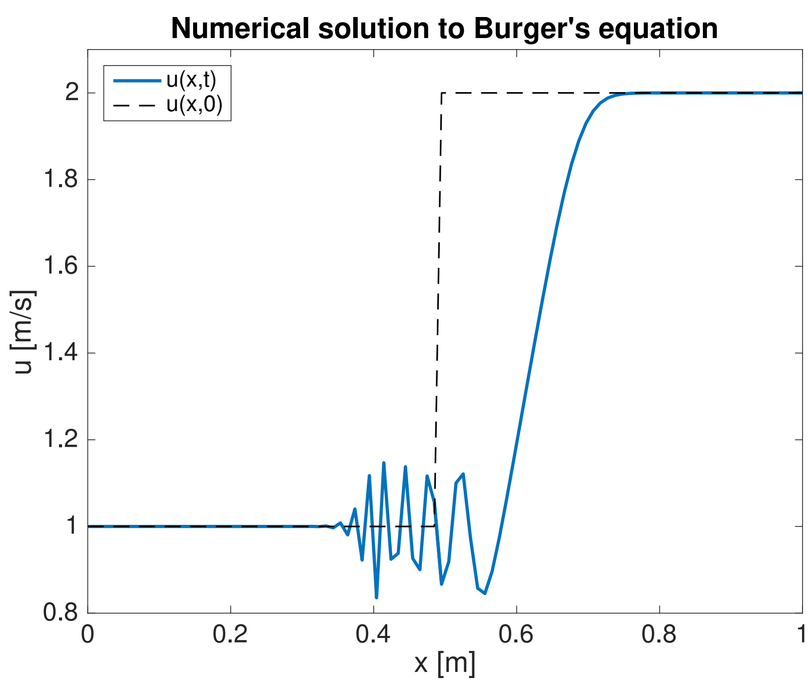

Figure 2.4: *Numerical solution to Burger's equation in Equation* (2.8) *using initial condition* $u_(x,0) = 1 + \Theta(x - 0.5)$. *We see that oscillations start at the lower boundary of the discontinuity and diffusion at the upper boundary.*

Instead of using the flux functions $\mathbf{F}_{i+1/2}$ used in Equation (2.12) we can instead use a fluctuation form proposed in [4] and later in [7] defined as

$$\frac{d\mathbf{w}}{dt} + \frac{1}{\Delta x}\left(\mathbf{D}^{+}_{i-1/2} + \mathbf{D}^{-}_{i+1/2}\right) = 0. \tag{2.17}$$

where $\mathbf{D}^{\pm}(\tilde{\mathbf{w}}_{i+1}, \tilde{\mathbf{w}}_i) : \mathbb{R}^n \times \mathbb{R}^n \to \mathbb{R}^n$. The fluctuations forms has to satisfy the condtion $\mathbf{D}^{\pm}(\tilde{\mathbf{w}}, \tilde{\mathbf{w}}) = 0$ and be Lipshitz continuous.

2.4 Path Consistency and Entropy Conservation

In the previous sections we saw that simple numerical methods can result in oscillating solutions and studying weak solutions can give unphysical results. In order to get a physically correct solution we need to be able to express the product $A(\tilde{\mathbf{w}})\tilde{\mathbf{w}}_x$ at the discontinuity. This is done using a path $\Phi : [0,1] \times \mathbb{R}^n \times \mathbb{R}^n \to \mathbb{R}^n$ which is also a C^1 function that requires

$$\begin{aligned}
\Phi(0, \tilde{\mathbf{w}}_-, \tilde{\mathbf{w}}_+) &= \tilde{\mathbf{w}}_- \\
\Phi(1, \tilde{\mathbf{w}}_-, \tilde{\mathbf{w}}_+) &= \tilde{\mathbf{w}}_+ \\
\Phi(s, \tilde{\mathbf{w}}, \tilde{\mathbf{w}}) &= \tilde{\mathbf{w}}.
\end{aligned} \tag{2.18}$$

Using this path we can formulate a weak solution to any hyperbolic system as long as it satisfies the Rankine-Hugonoit condition

$$\sigma \left[\!\left[\tilde{\mathbf{w}}\right]\!\right] = \int_0^1 A(\Phi(s, \tilde{\mathbf{w}}_-, \tilde{\mathbf{w}}_+))\Phi_s(s, \tilde{\mathbf{w}}_-, \tilde{\mathbf{w}}_+)ds \tag{2.19}$$

where σ is the shock speed and $\left[\!\left[\tilde{\mathbf{w}}\right]\!\right] = \tilde{\mathbf{w}}_+ - \tilde{\mathbf{w}}_-$. If we have a conservative system where $A = \nabla_{\mathbf{w}}\mathbf{f}$ the Rankine-Hugonoit relation is reduced to

$$\begin{aligned}
\sigma \left[\!\left[\tilde{\mathbf{w}}\right]\!\right] &= \int_0^1 A(\Phi(s, \tilde{\mathbf{w}}_-, \tilde{\mathbf{w}}_+))\Phi_s(s, \tilde{\mathbf{w}}_-, \tilde{\mathbf{w}}_+)ds \\
&= \int_0^1 \nabla_{\mathbf{w}}\mathbf{f}(\Phi(s, \tilde{\mathbf{w}}_-, \tilde{\mathbf{w}}_+))\Phi_s(s, \tilde{\mathbf{w}}_-, \tilde{\mathbf{w}}_+)ds \\
&= \int_0^1 \mathbf{f}_s(\Phi(s, \tilde{\mathbf{w}}_-, \tilde{\mathbf{w}}_+)ds. \\
&= \left[\!\left[\mathbf{f}\right]\!\right].
\end{aligned} \tag{2.20}$$

The path is tied to the numerical scheme by imposing path consistency

$$\mathbf{D}^{-}(\tilde{\mathbf{w}}_-, \tilde{\mathbf{w}}_+) + \mathbf{D}^{+}(\tilde{\mathbf{w}}_-, \tilde{\mathbf{w}}_+) = \int_0^1 A(\Phi(s, \tilde{\mathbf{w}}_-, \tilde{\mathbf{w}}_+))\Phi_s(s, \tilde{\mathbf{w}}_-, \tilde{\mathbf{w}}_+)ds \tag{2.21}$$

or simply

$$\mathbf{D}^-(\tilde{\mathbf{w}}_-, \tilde{\mathbf{w}}_+) + \mathbf{D}^+(\tilde{\mathbf{w}}_-, \tilde{\mathbf{w}}_+) = [\![\mathbf{f}]\!] \tag{2.22}$$

for a conservative system which has no dependence on the chosen path.

Besides path consistency we also need entropy conditions in order to get physical solutions where entropy refers to mathematical entropy which tend to zero over time rather than infinity. Entropy conditions are based on the existence of an entropy pair (η, q) where we have a convex entropy function $\eta : \mathbb{R}^n \to \mathbb{R}$ and an entropy flux function $q : \mathbb{R}^n \to \mathbb{R}$. If we multiply the hyperbolic system in Equation (2.1) with $\nabla_{\tilde{\mathbf{w}}}\eta$ from the left we get the entropy equality

$$\begin{aligned} \tilde{\mathbf{w}}_t + A(\tilde{\mathbf{w}})\tilde{\mathbf{w}}_x &= 0 \\ \nabla_{\tilde{\mathbf{w}}}\eta\tilde{\mathbf{w}}_t + \nabla_{\tilde{\mathbf{w}}}\eta A(\tilde{\mathbf{w}})\tilde{\mathbf{w}}_x &= 0 \\ \eta_t + q_x &= 0 \end{aligned} \tag{2.23}$$

where the entropy flux function has to satisfy the relation

$$\mathbf{v}A = \nabla_{\tilde{\mathbf{w}}} q \tag{2.24}$$

and $\mathbf{v}$ are the entropy variables defined as $\mathbf{v} = \nabla_{\tilde{\mathbf{w}}}\eta$.

An entropy pair (η, q) that satisfies Equation (2.23) for a hyperbolic system with fluctuation flux functions $\mathbf{D}^{\pm}$ that also satisfies

$$\mathbf{v}_-^T\mathbf{D}^-(\tilde{\mathbf{w}}_-, \tilde{\mathbf{w}}_+) + \mathbf{v}_+^T\mathbf{D}^+(\tilde{\mathbf{w}}_-, \tilde{\mathbf{w}}_+) = [\![q]\!] \tag{2.25}$$

is considered entropy conservative. Using the path consistency criteria in Equation (2.21) we can also write (2.25) as

$$\mathbf{v}_-^T \int_0^1 A(\Phi(s, \tilde{\mathbf{w}}_-, \tilde{\mathbf{w}}_+))\Phi_s(s, \tilde{\mathbf{w}}_-, \tilde{\mathbf{w}}_+)ds + [\![\mathbf{v}^T]\!]\, \mathbf{D}^+(\tilde{\mathbf{w}}_-, \tilde{\mathbf{w}}_+) = [\![q]\!] \tag{2.26}$$

which we can use to calculate Entropy Conservative Path Consistent (ECPC) schemes as defined below.

A numerical scheme according to Equation (2.17) to a hyperbolic system either conservative or non-conservative defined in Equations (2.2) and (2.1) respectively will be considered ECPC if it satisfies the path consistency conditions in Equation (2.19) and the entropy conservative condition in Equation (2.25). If the system is conservative according to Equation (2.2) and Equation (2.17) is a valid ECPC scheme we can construct an ECPC scheme using the flux function $\mathbf{F}$ in Equation (2.12). By setting

$$\begin{aligned} \mathbf{F} &= \mathbf{f}_- + \mathbf{D}^- \\ &= \mathbf{f}_+ - \mathbf{D}^+ \end{aligned} \tag{2.27}$$

and inserting Equation (2.22) into (2.25) we get

$$\begin{aligned}
\mathbf{v}_-^T\mathbf{D}^- + \mathbf{v}_+^T\mathbf{D}^+ &= [\![q]\!] \\
\mathbf{v}_-^T [\![\mathbf{f}]\!] + [\![\mathbf{v}^T]\!] \mathbf{D}^+ &= [\![q]\!] \\
\mathbf{v}_-^T [\![\mathbf{f}]\!] + [\![\mathbf{v}^T]\!] \left(\mathbf{f}_- - \mathbf{F}\right) &= [\![q]\!] \\
[\![\mathbf{v}^T]\!] \mathbf{F} &= [\![\mathbf{v}^T\mathbf{f}]\!] - [\![q]\!] \\
[\![\mathbf{v}^T]\!] \mathbf{F} &= [\![\psi]\!]
\end{aligned} \tag{2.28}$$

where ψ is the entropy potential. As can be seen in Equation (2.22) the choice of path does not affect the path consistency criteria but we still require that $\mathbf{D}(\mathbf{w}, \mathbf{w}) = 0$ which means

$$\mathbf{F}(\mathbf{w}, \mathbf{w}) = \mathbf{f}(\mathbf{w}). \tag{2.29}$$

To summarize we have that Equation (2.12) is a valid ECPC scheme if the system is conservative and the flux function $\mathbf{F}$ satisfies the simplified entropy conservation and path consistency criteria in Equation (2.28) and (2.29) respectively.

2.5 Entropy Stable Systems

The entropy equality in Equation (2.23) is only valid for smooth solutions for Equation (2.1) since it states that entropy is conserved but in the presence of shocks entropy actually dissipates since physical entropy would increase. To get dissipation we use the vanishing viscosity method by adding a parabolic term to our system resulting in

$$\tilde{\mathbf{w}}_t^\mu + A(\tilde{\mathbf{w}}^\mu)\tilde{\mathbf{w}}_x^\mu = \mu\tilde{\mathbf{w}}_{xx}. \tag{2.30}$$

If we have a non-conservative system our results may not converge towards physical results if the viscosity operator is a single Laplace operator. If there is a transformation matrix T that transforms a conservative system to our non-conservative system we can multiply to the right of the Laplace operator and it will yield the correct non-conservative viscosity operator.

For the system in Equation (2.1) to yield physical results we require that $\tilde{\mathbf{w}} = \lim_{\mu\to 0} \tilde{\mathbf{w}}^\mu$. Similar to how we derived the entropy equality we again multiply Equation (2.30) with $\nabla_{\tilde{\mathbf{w}}}\eta^\mu$ from the left which results in

$$\begin{aligned}
\nabla_{\tilde{\mathbf{w}}}\eta^\mu\tilde{\mathbf{w}}_t^\mu + \nabla_{\tilde{\mathbf{w}}}\eta^\mu A(\tilde{\mathbf{w}}^\mu)\tilde{\mathbf{w}}\mu_x &= \nabla_{\tilde{\mathbf{w}}}\eta^\mu\mu\tilde{\mathbf{w}}_{xx} \\
\eta_t^\mu + q_x^\mu &= \mu\eta_{xx}^\mu - \mu\nabla^2\eta^\mu\left(\tilde{\mathbf{w}}_x^\mu\right)^2 \\
\eta_t^\mu + q_x^\mu &\le \mu\eta_{xx}^\mu
\end{aligned} \tag{2.31}$$

where we used that η is a convex function which means $\nabla^2\eta > 0 \; \forall \tilde{\mathbf{w}}$. Now we can take the vanishing viscosity limit $\mu \to 0$ which results in the entropy inequality

$$\eta_t + q_x \leq 0. \tag{2.32}$$

Adding a numerical viscosity operator to the scheme we transform our scheme to an Entropy Stable Path Consistent (ESPC) scheme. Compared to non-ECPC schemes we have that ECPC schemes add no numerical viscosity which means we can choose a viscosity operator that mimics actual physical viscosity. We use a second order discretization for the viscosity operator yielding

$$\begin{aligned} \tilde{\mathbf{w}}_x &= \frac{\tilde{\mathbf{w}}_{j+1} - \tilde{\mathbf{w}}_{j-1}}{2\Delta x} \\ \tilde{\mathbf{w}}_{xx} &= \frac{\tilde{\mathbf{w}}_{j+1} - 2\tilde{\mathbf{w}}_j + \tilde{\mathbf{w}}_{j-1}}{\Delta x^2} \end{aligned} \tag{2.33}$$

which means that the viscosity operator is inversely proportional to Δx^2 instead of Δx. This means that by decreasing the mesh size the effects of the viscosity operator will become more significant. The last part of choosing the diffusion operator is assigning a value to μ and while choosing the actual physical value would be appropriate it is often of to low value that. In order to get proper diffusion we thus need a mesh that is so fine that any computation will simply take too long for it to be viable. In [8] it is shown that we can increase the value of μ and still have the same effects as physical diffusion and one common choice is the Lax-Friedrichs operator which is

$$\mu = \frac{c_{max}\Delta x}{2} \tag{2.34}$$

where c_{max} is the speed of sound for the state $\tilde{\mathbf{w}}$. Another more accurate choice would be the Rusanov operator in which c_{max} is replaced by the local speed of sound for each interface between two mesh points. Both of these operators scale with Δx meaning that our diffusion operator is now also inversely proportional to Δx which means that the solution will no longer be affected by the choice in mesh size.

2.6 Time Discretization

Up to now we have focused solely on the discretization of the space derivatives but in order to implement the scheme we will also need to choose a discretization of the derivative with respect to time. The simplest choice would be a standard Euler forward method where

$$\begin{aligned} \frac{d\tilde{\mathbf{w}}}{dt} &= -A(\tilde{\mathbf{w}})\tilde{\mathbf{w}}_x \\ \tilde{\mathbf{w}}^{n+1} &= \tilde{\mathbf{w}}^n - \Delta t A(\tilde{\mathbf{w}}^n)\tilde{\mathbf{w}}_x^n \end{aligned} \tag{2.35}$$

but it is only first order accurate. A more prudent choice would be using Heun's method which is a second order accurate method originating from the Runge-Kutta method. It is done by first calculating a transitional step using the Euler forward method

$$\tilde{\mathbf{w}}^{n+1,*} = \tilde{\mathbf{w}}^n - \Delta t A(\tilde{\mathbf{w}}^n)\tilde{\mathbf{w}}_x^n \tag{2.36}$$

and then using that to calculate $\tilde{\mathbf{w}}^{n+1}$ by

$$\tilde{\mathbf{w}}^{n+1} = \tilde{\mathbf{w}}^n - \frac{\Delta t}{2}\Bigg(A(\tilde{\mathbf{w}}^n)\tilde{\mathbf{w}}_x^n + A(\tilde{\mathbf{w}}^{n+1,*})\tilde{\mathbf{w}}_x^{n+1,*}\Bigg). \tag{2.37}$$

With the choice of discretization we also need to determine that our system is stable which is done by studying the Courant-Friedrich-Lewy condition which is

$$\frac{s_{max}\Delta t}{\Delta x} = C. \tag{2.38}$$

where s_{max} is the highest eigenvalue in the system and $C \leq 1$ is known as the Courant number. Any viable Courant number will solve the system but a higher number will reduce simulation time at the expense of precision of the results. A non-viable Courant number will prevent the system from converging and instead oscillate out of control yielding unphysical results. This stability criteria can be explained by studying the systems wave speed which is represented by s_{max}. For $C > 1$ we will calculate wave amplitudes further away than the wave could have possibly travelled.

Chapter 3

Defining Two-phase Entropy Stable Schemes

In this chapter we will use the theory presented in the previous chapter on a hyperbolic system based on the two fluid model. While most of the system is clearly defined the pressure term can be chosen more freely and in this thesis we study three systems with different pressure definitions. The first two are based on previously studied one phase systems and will mostly be used as a comparison for the last which is a previously unstudied two phase expression for the pressure. Finally we create ESPC schemes for all three systems using the theory from the previous chapter.

3.1 Two-Fluid Model

The two-fluid model we use consists of the balance laws for mass and momentum. If the fluid is heated we also need to add a third balance law choosing between energy, enthalpy or temperature as we can easily transform between them. The balance law for mass is the continuity equation

$$\left(\alpha_k \rho_k\right)_t + \left(\alpha_k \rho_k v_k\right)_x + M_{ki} = 0 \tag{3.1}$$

where α_k is the volume fraction of phase k, ρ_k is density, v_k is velocity, and M_{ki} is the jump interface condition representing transfer between phases inside the control volume. The balance law for momentum is based on Newton's second law of motion and is defined as

$$\Big(\alpha_k\rho_k v_k\Big)_t + \Big(\alpha_k\rho_k v_k^2\Big)_x + \alpha_k P_{k,x} + F_{ki} = \alpha_k\rho_k g_x \tag{3.2}$$

where P_k is pressure, F_{ki} is the jump interface condition, and g is gravity.

The mass and momentum equations for the two-fluid model are written as

$$\begin{aligned}
\Big(\alpha\rho_v\Big)_t + \Big(\alpha\rho_v u_v\Big)_x + M_{vi} &= 0\\
\Big((1-\alpha)\rho_l\Big)_t + \Big((1-\alpha)\rho_l u_l\Big)_x + M_{li} &= 0\\
\Big(\alpha\rho_v u_v\Big)_t + \Big(\alpha\rho_v u_v^2\Big)_x + \alpha P_{v,x} + F_{vi} &= \alpha\rho_v g_x\\
\Big((1-\alpha)\rho_l u_l\Big)_t + \Big((1-\alpha)\rho_l u_l^2\Big)_x + (1-\alpha)P_{l,x} + F_{li} &= (1-\alpha)\rho_l g_x
\end{aligned} \tag{3.3}$$

similar to [9]. We now add the two momentum equations which yields

$$\begin{aligned}
\Big(\alpha\rho_v\Big)_t + \Big(\alpha\rho_v u_v\Big)_x + M_{vi} &= 0\\
\Big((1-\alpha)\rho_l\Big)_t + \Big((1-\alpha)\rho_l u_l\Big)_x + M_{li} &= 0\\
\Big(\alpha\rho_v u_v + (1-\alpha)\rho_l u_l\Big)_t + \Big(\alpha\rho_v u_v^2 + (1-\alpha)\rho_l u_l^2\Big)_x + \alpha P_{v,x} + (1-\alpha)P_{l,x} + F_{vi} + F_{li} &=\\
\alpha\rho_v g_x + (1-\alpha)\rho_l g_x&.
\end{aligned} \tag{3.4}$$

Transfer of momentum from one phase to the other is the same as a negative transfer of momentum from the latter to the former so we have that

$$F_{vi} + F_{li} = 0. \tag{3.5}$$

Now we will do a few approximations where we assume that there is no transfer of mass between phases i.e $M_{li} = M_{vi} = 0$, we neglect any effect from gravity, slip ratio is equal to unity i.e $u_l = u_v$, and finally we will assume equal pressure in both phases which is a common approximation in two-phase models. Combining all of these results in

$$\begin{aligned}
\Big(\alpha\rho_v\Big)_t + \Big(\alpha\rho_v u\Big)_x &= 0\\
\Big((1-\alpha)\rho_l\Big)_t + \Big((1-\alpha)\rho_l u\Big)_x &= 0\\
\Big(\alpha\rho_v u\Big)_t + \Big((1-\alpha)\rho_l u\Big)_t + \Big(\alpha\rho_v u^2\Big)_x + \Big((1-\alpha)\rho_l u^2\Big)_x + P_x &= 0
\end{aligned} \tag{3.6}$$

and defining vapour density $\alpha\rho_v = n$ and liquid density $(1-\alpha)\rho_l = m$ we get

$$\begin{aligned}
n_t + \Big(nu\Big)_x &= 0\\
m_t + \Big(mu\Big)_x &= 0\\
\Big((m+n)u\Big)_t + \Big((m+n)u^2\Big)_x + P_x &= 0.
\end{aligned} \tag{3.7}$$

Studying Equation (3.7) we see that depending on how we choose to express the pressure P will affect the model. In this thesis we will study an isothermal (constant temperature), isentropic (constant entropy), and finally one based on the adiabatic process.

3.2 Isothermal System

We begin by setting $M = m + n$ and $P = c^2 M$ where c is the speed of sound which results in

$$\begin{aligned} m_t + \Big(mu\Big)_x &= 0 \\ M_t + \Big(Mu\Big)_x &= 0 \\ \Big(Mu\Big)_t + \Big(Mu^2\Big)_x + c^2 M_x &= 0. \end{aligned} \tag{3.8}$$

with $\mathbf{w} = (m, M, Mu)$ and $\mathbf{f} = (mu, Mu, Mu^2 + c^2 M)$. From this we can see that the last two equations are the Euler equations which are the Navier-Stokes equations but with the simplification of neglecting the effects of viscosity. Using the chain rule we can simplify the system into

$$\begin{aligned} m_t + \Big(mu\Big)_x &= 0 \\ M_t + \Big(Mu\Big)_x &= 0 \\ u_t + \left(\frac{u^2}{2} + c^2 \log M\right)_x &= 0 \end{aligned} \tag{3.9}$$

with $\tilde{\mathbf{w}} = (m, M, u)$ and

$$A = \begin{bmatrix} u & 0 & m \\ 0 & u & M \\ 0 & \frac{c^2}{M} & u \end{bmatrix} \tag{3.10}$$

and even though we can write the system in divergence form u is not a conserved variable which will be seen when we add diffusion. From this we can verify that the system is hyperbolic by calculating the eigenvalues of A by

$$\det\Big(A - \lambda I\Big) = 0 \Rightarrow \begin{aligned} \lambda_1 &= u \\ \lambda_{2,3} &= u \pm c \end{aligned} \tag{3.11}$$

which are real and distinct which means the system is hyperbolic. The next step is to define the entropy pair (η, q) and we begin by selecting the entropy function η as the total energy in the system

$$\eta(\tilde{\mathbf{w}}) = \frac{Mu^2}{2} + c^2 M \log M \tag{3.12}$$

which has the entropy variables

$$\mathbf{v}(\tilde{\mathbf{w}}) = \nabla_{\tilde{\mathbf{w}}}\eta = \left(0, \frac{u^2}{2} + c^2 \log M + c^2, Mu\right). \tag{3.13}$$

Using the entropy equality in Equation (2.23) we get the entropy flux q which becomes

$$\begin{aligned} q_x &= -\eta_t \\ &= -\left(\frac{u^2}{2}M_t + Muu_t + c^2 M_t \log M + c^2 M_t\right) \\ &= \left(\frac{Mu^3}{2} + Muc^2 \log M + Muc^2\right)_x \\ q &= \frac{Mu^3}{2} + Muc^2 \log M + Muc^2 \end{aligned} \tag{3.14}$$

where the time derivatives are replaced with spatial derivatives using the system in Equation (3.9). Before we can calculate the numerical scheme we need to choose a path and for this system we choose a linear path for all three variables i.e

$$\begin{aligned} m(s) &= m_- + s\left(m_+ - m_-\right) \\ M(s) &= M_- + s\left(M_+ - M_-\right) \\ u(s) &= u_- + s\left(u_+ - u_-\right) \end{aligned} \tag{3.15}$$

and we continue by calculating the integrals along the path

$$\begin{aligned} \mathbf{J} &= \int_0^1 A(\Phi(s, \tilde{\mathbf{w}}_-, \tilde{\mathbf{w}}_+))\Phi_s(s, \tilde{\mathbf{w}}_-, \tilde{\mathbf{w}}_+)ds \\ &= \Bigg(\int_0^1 u(s)\frac{dm(s)}{ds}ds + \int_0^1 m(s)\frac{du(s)}{ds}ds, \\ &\quad \int_0^1 u(s)\frac{dM(s)}{ds}ds + \int_0^1 M(s)\frac{du(s)}{ds}ds, \\ &\quad \int_0^1 \frac{c^2}{M(s)}\frac{dM(s)}{ds}ds + \int_0^1 u(s)\frac{du(s)}{ds}ds \Bigg) \\ &= \left([\![mu]\!], [\![Mu]\!], c^2 [\![\log M]\!] + \bar{u}[\![u]\!] \right). \end{aligned} \tag{3.16}$$

where we used the identity $[\![AB]\!] = \bar{A}\,[\![B]\!] + \bar{B}\,[\![A]\!]$. Inserting this into Equation (2.26) we get

$$\begin{aligned} \mathbf{v}_-^T\mathbf{J} + [\![\mathbf{v}^T]\!]\,\mathbf{D}^+(\tilde{\mathbf{w}}_-, \tilde{\mathbf{w}}_+) &= [\![q]\!] \\ \left[\!\!\left[\left(0, \frac{u^2}{2} + c^2\log M + c^2, Mu\right)\right]\!\!\right]\mathbf{D}^+(\tilde{\mathbf{w}}_-, \tilde{\mathbf{w}}_+) &= \left[\!\!\left[\frac{u^2}{2}\right]\!\!\right][\![Mu]\!] + c^2\,[\![\log M]\!]\,[\![Mu]\!]\,. \end{aligned} \tag{3.17}$$

This results in the numerical flux function

$$\mathbf{D}^+(\tilde{\mathbf{w}}_-, \tilde{\mathbf{w}}_+) = \frac{1}{2}\left([\![mu]\!]\,, [\![Mu]\!]\,, \left[\!\!\left[\frac{u^2}{2}\right]\!\!\right] + [\![c^2\log M]\!]\right) \tag{3.18}$$

where the first element could be chosen freely and set to $[\![mu]\!]/2$ because of symmetry while fulfilling the path consistency criteria. With $\mathbf{D}^+$ we can calculate $\mathbf{D}^-$ with

$$\begin{aligned} \mathbf{D}^+ + \mathbf{D}^- &= \mathbf{J} \\ \mathbf{D}^- &= \frac{1}{2}\left([\![mu]\!]\,, [\![Mu]\!]\,, \left[\!\!\left[\frac{u^2}{2}\right]\!\!\right] + [\![c^2\log M]\!]\right). \end{aligned} \tag{3.19}$$

The last step is to add the viscosity operator and since this system is not conservative we will add the viscosity operator $\mu T\mathbf{w}_{xx}$ where the transformation matrix is

$$T = \begin{bmatrix} 1 & 0 & 0 \\ 0 & 1 & 0 \\ 0 & -\frac{u}{M} & \frac{1}{M} \end{bmatrix}. \tag{3.20}$$

The resulting viscosity operator thus becomes

$$\mu T\mathbf{w}_{xx} = \mu\Big(m_{xx}, M_{xx}, u_{xx} + 2(\log M)_x u_x\Big) \tag{3.21}$$

and since the second term in the last element can not be written in divergence form the system is considered non-conservative. It is also shown in [10] that the system will not converge to a physical solution as $\mu \to 0$ if we only add a Laplace operator i.e. μu_{xx} which means that u is not a conserved variable.

3.3 Isentropic System

Similar to the previous system we begin by setting $M = m + n$ which results in the system

$$\begin{aligned} m_t + \Big(mu\Big)_x &= 0 \\ M_t + \Big(Mu\Big)_x &= 0 \\ \Big(Mu\Big)_t + \Big(Mu^2\Big)_x + P_x &= 0 \end{aligned} \tag{3.22}$$

and while for the previous system we had an expression for the pressure fit for single phase liquid this time we will use single phase gas by setting the pressure $P(M) = KM^\gamma$ where γ is the adiabatic index. This time we will use a conservative approach by setting $\xi = Mu$ and $\mathbf{w} = (m, M, \xi)$ which yields the system

$$\begin{aligned} m_t + \left(\frac{m\xi}{M}\right)_x &= 0 \\ M_t + \xi_x &= 0 \\ \xi_t + \left(\frac{\xi^2}{M}\right)_x + P_x &= 0 \end{aligned} \tag{3.23}$$

where $\mathbf{f} = \left(\frac{m\xi}{M}, \xi, \frac{\xi^2}{M} + P\right)$. Similar to last time we set the entropy function to the total energy of the system which is

$$\eta = \frac{\xi^2}{2M} + \frac{P}{\gamma - 1}. \tag{3.24}$$

We calculate the entropy variables and entropy flux as we did for the previous system and we get

$$\mathbf{v} = \left(0, -\frac{\xi^2}{2M^2} + \frac{P_M}{\gamma - 1}, \frac{\xi}{M}\right) \tag{3.25}$$

and

$$q = \frac{\xi^3}{2M^2} + \frac{\xi P}{\gamma - 1}. \tag{3.26}$$

Since the system described by Equation (3.23) is conservative we can use the simpler approach to get a numerical scheme and we start by calculating the entropy potential which is

$$\begin{aligned} \psi &= \mathbf{v}^T\mathbf{f} - q \\ &= -\frac{\xi^3}{2M^2} + \frac{\xi P_M}{\gamma - 1} + \frac{\xi^3}{M^2} + \frac{\xi P}{M} - \frac{\xi^3}{2M^2} - \frac{\xi P_M}{\gamma - 1} \\ &= \frac{\xi P}{M}. \end{aligned} \tag{3.27}$$

We can now insert this into Equation (2.28) which yields

$$K \left[\!\left[\frac{\gamma}{\gamma-1} M^{\gamma-1} \right]\!\right] F_2 - \overline{\frac{\xi}{M}} \left[\!\left[\frac{\xi}{M} \right]\!\right] F_2 + \left[\!\left[\frac{\xi}{M} \right]\!\right] F_3 = K \left[\!\left[\frac{\xi}{M} M^{\gamma} \right]\!\right] \tag{3.28}$$

and as before the equation is not dependent on F_1 which means that it can be chosen freely. The adiabatic index γ is defined as

$$\gamma = \frac{\beta+2}{\beta} \tag{3.29}$$

where β is the degrees of freedom which means we can rewrite Equation (3.28) as

$$K \left[\!\left[\frac{\beta+2}{2} M^{2/\beta} \right]\!\right] F_2 - \overline{\frac{\xi}{M}} \left[\!\left[\frac{\xi}{M} \right]\!\right] F_2 + \left[\!\left[\frac{\xi}{M} \right]\!\right] F_3 = K \left[\!\left[\frac{\xi}{M} M^{1+2/\beta} \right]\!\right]. \tag{3.30}$$

Using the identity

$$[\![AB]\!] = \overline{A}\,[\![B]\!] + \overline{B}\,[\![A]\!] \tag{3.31}$$

we can group the equation into kinetic and pressure differences which yields the system

$$\begin{aligned} F_3 - K\overline{M^{\gamma}} - \overline{\frac{\xi}{M}} F_2 &= 0 \\ 2\frac{\beta+2}{2}\overline{M^{1/\beta}}\,\left[\!\left[M^{1/\beta} \right]\!\right] F_2 - \overline{\frac{\xi}{M}}\,\left[\!\left[M^{1+2/\beta} \right]\!\right] &= 0. \end{aligned} \tag{3.32}$$

Since the second equation only depends on F_2 we can solve that first and insert it into the first equation to calculate F_3. The only problem is the term $\left[\!\left[M^{1/\beta} \right]\!\right]$ which can result in division by zero if we just try to solve the equation for F_3. Instead we are going to use

$$\left[\!\left[M^{k/\beta} \right]\!\right] = \Omega(k,\beta)\,\left[\!\left[M^{1/\beta} \right]\!\right],\ \Omega(k,\beta) = \sum_{i=0}^{k-1} \overline{M^{i/\beta}}\,\overline{M^{1/\beta}}^{k-1-i} \tag{3.33}$$

which can be shown using the identity in Equation (3.31). We can now use the identity in Equation (3.33) into the second equation in Equation (3.32) which results in

$$\begin{aligned} F_2 &= \frac{\overline{\frac{\xi}{M}}\Omega(\beta+2,\beta)}{(\beta+2)\overline{M^{1/\beta}}} \\ F_3 &= F_2\overline{\frac{\xi}{M}} + K\overline{M^{\gamma}}. \end{aligned} \tag{3.34}$$

This scheme is entropy conservative and if we can also prove that it is path conservative it is a valid ECPC-scheme. Since this a conservative system we only require $\mathbf{F}(\mathbf{w},\mathbf{w}) =$

$\mathbf{f}$ and we do not have to choose a specific path since they are all valid. When $\mathbf{w}_+ = \mathbf{w}_-$ we have that $\overline{A} = A$, $[\![A]\!] = 0$, and $\Omega(\beta+2,\beta) = (\beta+2)M^{1+1/\beta}$. Regarding F_1 we can choose it freely and be entropy conservative so with all of this we have that

$$\begin{aligned} F_1 &= \frac{m\xi}{M} \\ F_2 &= \xi \\ F_3 &= \frac{\xi^2}{M} + P \end{aligned} \tag{3.35}$$

which shows that $\mathbf{F}(\mathbf{w},\mathbf{w}) = \mathbf{f}$ meaning that our scheme is both entropy conservative and path consistent and thus ECPC. The last step is to add numerical diffusion to the system and since the system is conservative we simply add a Laplace term to each variable making the viscosity operator

$$\mu\mathbf{w}_{xx} = \mu(m_{xx}, M_{xx}, \xi_{xx}). \tag{3.36}$$

3.4 Adiabatic Process

The last system we are going to study is another conservative system but this time we are going to use the approximation that $m \gg n$ which means $m + n \approx m$. This is a valid approximation since $\rho_l \gg \rho_v$ and if α is so close to unity that $m \approx n$ we can simply use a one-phase system. By also setting $\xi = mu$ we get the conservative system

$$\begin{aligned} m_t + \xi_x &= 0 \\ n_t + \left(\frac{n\xi}{m}\right)_x &= 0 \\ \xi_t + \left(\frac{\xi^2}{m}\right)_x + P_x &= 0 \end{aligned} \tag{3.37}$$

with $\mathbf{w} = (m, n, \xi)$ and $\mathbf{f} = \left(\xi, \frac{n\xi}{m}, \frac{\xi^2}{m} + P\right)$. The previous two systems we studied used an expression for pressure originating from single phase systems but this time we will use two-phase model. The pressure for the gas phase is determined using the adiabatic process which means

$$P = K\rho_v^\gamma \tag{3.38}$$

and since we have assumed equal pressure we know that the pressure for the liquid phase is equal to this. Using our expressions for the variables m and n we can derive an expression for the pressure as

$$\begin{aligned} P(m,n) &= K\rho_v^\gamma \\ &= K\left(\frac{n}{\alpha}\right)^\gamma \\ &= K\left(\frac{\rho_l n}{\rho_l - m}\right)^\gamma . \end{aligned} \tag{3.39}$$

The derivation of the ECPC-scheme is the same as before where we first define the entropy function as the total energy in the system

$$\eta = \frac{\xi^2}{2m} + Q(m,n)\,,\; Q(m,n) = \int_0^1 \frac{P(sm,sn)}{s^2} ds = \frac{P}{\gamma - 1}\left(1 - \frac{m}{\rho_l}\right). \tag{3.40}$$

where we use the expression of potential energy due to pressure from [11]. The entropy variables thus become

$$\mathbf{v} = \left(-\frac{\xi^2}{2m^2} + Q_m, Q_n, \frac{\xi}{m}\right) \tag{3.41}$$

and the entropy flux becomes

$$q = \frac{\xi^3}{2m^2} + \frac{\xi Q}{m} + \frac{\xi P}{m}. \tag{3.42}$$

Similar to the previous system we have that the entropy potential becomes

$$\psi = \frac{\xi P}{m} \tag{3.43}$$

and it can be shown that for any $P = P(m,n)$ the system will always have an entropy potential equal to the velocity times the pressure.

Now we can calculate the flux functions using Equation (2.28) which yields

$$\begin{aligned} \left[\!\left[\mathbf{v}^T\right]\!\right] \mathbf{F} &= [\![\psi]\!] \\ \left[\!\left[-\frac{\xi^2}{2m^2} + Q_m\right]\!\right] F_1 + [\![Q_n]\!] F_2 + \left[\!\left[\frac{\xi}{m}\right]\!\right] F_3 &= \left[\!\left[\frac{\xi P}{m}\right]\!\right] \end{aligned} \tag{3.44}$$

and again we separate the kinetic and pressure differences into two equations. This results in

$$\begin{aligned} -\overline{\frac{\xi}{m}} F_1 + F_3 - \overline{P} &= 0 \\ [\![Q_m]\!] F_1 + [\![Q_n]\!] F_2 - \overline{\frac{\xi}{m}} [\![P]\!] &= 0 \end{aligned} \tag{3.45}$$

with the derivatives Q_m and Q_n being

$$\begin{aligned} Q_m &= \frac{P}{\rho_l} \\ Q_n &= \frac{\beta+2}{2}\frac{\rho_l - m}{\rho_l n}P. \end{aligned} \tag{3.46}$$

Now we are going to make the assumption that the flux functions are

$$\begin{aligned} F_1 &= g(\beta, \mathbf{w})\overline{\frac{\xi}{m}} \\ F_2 &= g(\beta, \mathbf{w})\overline{\frac{n\xi}{m^2}} \\ F_3 &= g(\beta, \mathbf{w})\overline{\frac{\xi}{m}}^2 + \overline{P} \end{aligned} \tag{3.47}$$

for some function $g(\beta, \mathbf{w})$ and inserting this into Equation (3.45) yields

$$g(\beta, \mathbf{w})\overline{\frac{\xi}{m}}\,[\![Q_m]\!] + g(\beta, \mathbf{w})\overline{\frac{n\xi}{m^2}}\,[\![Q_n]\!] - \overline{\frac{\xi}{m}}\,[\![P]\!] = 0. \tag{3.48}$$

Setting $b = \rho_l n/(\rho_l - m)$ results in $P = Kb^\gamma$ and using the derivatives in Equation (3.46) we get

$$\frac{1}{\rho_l}g(\beta, \mathbf{w})\overline{\frac{\xi}{m}}\,[\![b^{1+2/\beta}]\!] + \frac{\beta+2}{2}g(\beta, \mathbf{w})\overline{\frac{n\xi}{m^2}}\,[\![b^{2/\beta}]\!] - \overline{\frac{\xi}{m}}\,[\![b^{1+2/\beta}]\!] = 0. \tag{3.49}$$

Now we can use the same approach as the previous system where

$$[\![b^{n/\beta}]\!] = \Omega(n, \beta)\,[\![b^{1/\beta}]\!]\ ,\ \Omega(n, \beta) = \sum_{i=0}^{n-1} \overline{b^{i/\beta}}\,\overline{b^{1/\beta}}^{n-1-i} \tag{3.50}$$

which results in

$$\frac{1}{\rho_l}g(\beta, \mathbf{w})\overline{\frac{\xi}{m}}\Omega(\beta+2, \beta) + (\beta+2)g(\beta, \mathbf{w})\overline{\frac{n\xi}{m^2}}\overline{b^{1/\beta}} - \overline{\frac{\xi}{m}}\Omega(\beta+2, \beta) = 0. \tag{3.51}$$

Solving this equation for the function $g(\beta, \mathbf{w})$ gives

$$g(\beta, \mathbf{w}) = \frac{\Omega(\beta+2, \beta)\overline{\frac{\xi}{m}}}{\frac{1}{\rho_l}\Omega(\beta+2, \beta)\overline{\frac{\xi}{m}} + (\beta+2)\overline{b^{1/\beta}}\,\overline{\frac{n\xi}{m^2}}} \tag{3.52}$$

and to fulfil the path consistency criteria we require that $g(\beta, \mathbf{w}) = m$ when $\mathbf{w}_- = \mathbf{w}_+$. For this case we have that

$$\Omega(n, \beta) = nb^{(n-1)/\beta} \tag{3.53}$$

which makes

$$\begin{aligned} g(\beta, \mathbf{w}) &= \frac{(\beta+2)b^{1+1/\beta}}{\frac{1}{\rho_l}(\beta+2)b^{1+1/\beta} + (\beta+2)b^{1/\beta}\frac{n}{m}} \\ &= \frac{\frac{\rho_l n}{\rho_l - m}}{\frac{n}{\rho_l - m} + \frac{n}{m}} \\ &= m \end{aligned} \tag{3.54}$$

which makes the numerical flux function $\mathbf{F}(\mathbf{w}, \mathbf{w}) = \mathbf{f}$. Since the scheme is also entropy conservative we have that the scheme in Equation (3.47) is ECPC. Finally we insert numerical diffusion to make the scheme ESPC. As the system is conservative we again add a Laplace term

$$\mu \mathbf{w}_{xx} = \mu(m_{xx}, n_{xx}, \xi_{xx}) \tag{3.55}$$

as the viscosity operator.

Chapter 4

Numerical Experiments & Analysis

In this chapter we will study the systems we defined in the previous chapter. We first take a quick look at the stability criteria and how it affects the solution. After this we study two different scenarios and see how the system responds. The first scenario is a replication of flow reversal due to increased void fraction and demonstrates how the system responds to a single discontinuity. The second one is where a finite region of the fluid has a decreased void fraction and shows how the system handles a two-sided discontinuity. For the purpose of all the tests the software Matlab was used.

4.1 Stability Investigation

In Section 2.6 we studied the requirements for stability in the system. Using the entropy conditions from [4] we created an ESPC scheme for the Burger's equation and tested different Courant numbers. The results can be seen in Figure 4.1 and we see that regardless of valid Courant number chosen the system converges to the same solution. Using a lower Courant number increases the runtime of the simulation due to each time step being shorter which we can see in Equation (2.38). For a non-valid Courant number we see that the system oscillates heavily even for a small increase and these oscillations will also increase over time. For the system in Figure 4.1 the system will oscillate until we reach the datatype limit causing Matlab to return NaN (Not a Number). For the ESPC schemes we defined in Chapter 3 the oscillations will cause imaginary numbers when one of the density terms becomes negative.

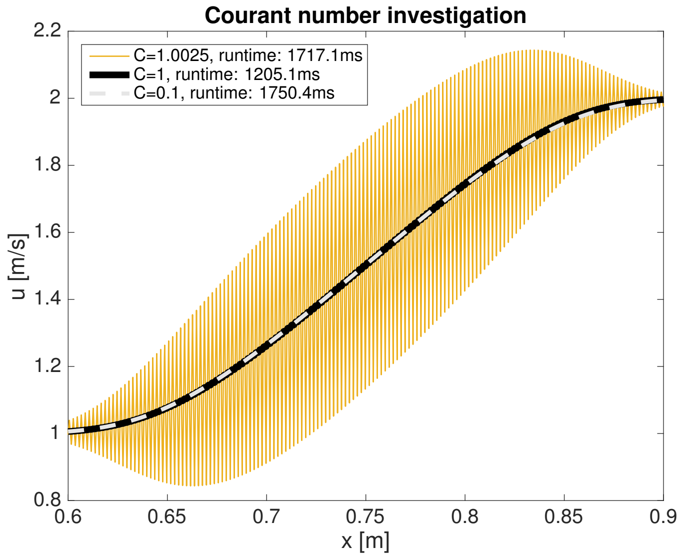

Figure 4.1: *Demonstration of the difference in Courant numbers for the Burger's equation. Valid Courant numbers makes the systems converge to the same solution which can be seen in the figure. Just increasing the Courant number by* 0.25% *above the maximum causes heavy oscillations which is seen in the figure. Changing the Courant number also affects the simulation runtime since it affects the size of each time step.*

4.2 One-sided Discontinuity

The first scenario studied in this thesis is a one-sided discontinuity where two fluids with different void fractions collide into each other and mix. This scenario represents a case of flow reversal where something has caused an increase in void fraction and the resulting increase in pressure results in a reversal of flow. First we study the difference between ECPC and ESPC schemes to show how the system is affected by adding numerical diffusion and the results can be seen in Figure 4.2. From the results we see that both schemes have the same general solution but with oscillations for the ECPC scheme and these increase in amplitude over time until m becomes larger than ρ_l which causes $P(m, n)$ to return imaginary numbers. In [10] it was shown that adding an incorrect viscosity operator the system could potentially converge towards an unphysical solution. Comparing the two schemes shows that this is not the case as both schemes have similar final amplitude and only a slight difference in how far the wave has travelled on the left side indicating a difference in wave speed. Studying each figure more closely starting with the liquid density in Figure 4.2a we see that as the two sides mix together they stabilize at a final amplitude and send out a shock wave at each side where the one on the right is often referred to as an expansion or rarefraction wave. The wave on the left is steeper than the right wave and this is caused by the overall movement of the fluid. In Figure 4.2b we see that the fluid velocity is negative which means it is moving to the left which causes the left wave to contract and the right wave to expand.

As our ESPC scheme for the adiabatic system has converged towards a physical solution we can now compare it to the two other systems defined in Chapter 3. The results can be seen in Figure 4.3 and we see that the results for the Euler and isentropic systems are similar while the adiabatic process system differs in both final amplitude and wave speed most notably towards the upper limit of the discontinuity. The reason for the difference in results is due to the fact that the systems react differently to changes in density and this is explained more thoroughly in Section 4.4.

The last example for this scenario is the adiabatic system when the two sides have different velocities. The initial velocities correspond to both fluids moving towards each other and the results can be seen in Figure 4.4. The results show that the initial velocity affects the final amplitude of the system. In this example the final amplitude of the liquid density seen in Figure 4.4a increases because the fluid from both sides has a higher initial velocity which means more come in to the middle and mix from both sides. In Figure 4.4b we see that the simulated region is mostly unaffected by the change in velocity.

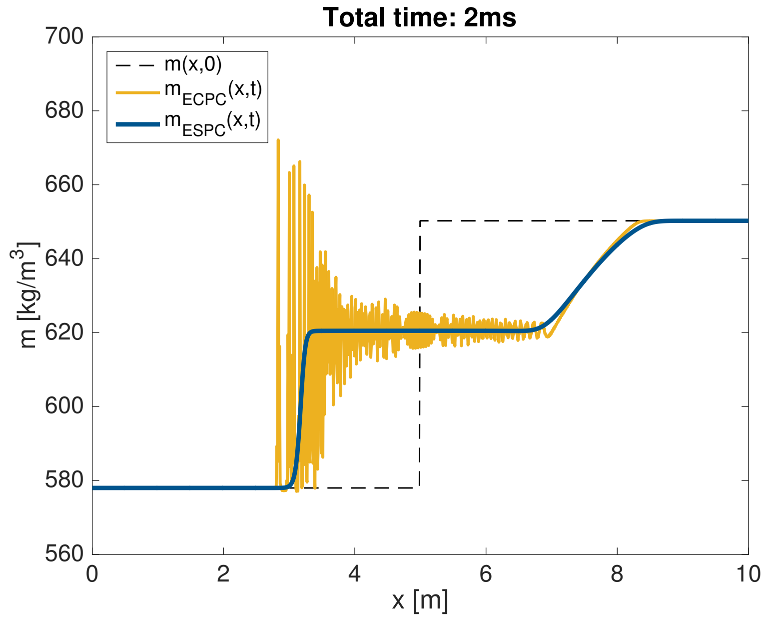

(a)

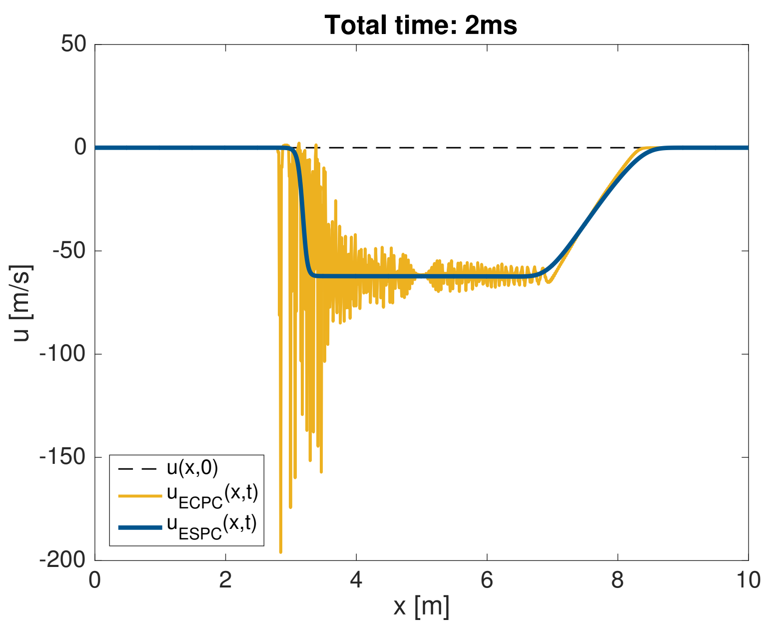

(b)

Figure 4.2: *Comparison between the ECPC and ESPC schemes for (a) liquid density m and (b) fluid velocity u. Both systems converge towards the same general solution sharing final amplitude and similar wave speeds with the exception of a small difference in wave speed of the wave moving to the left but the ECPC solution oscillates heavily. The oscillations will eventually cause the system to return imaginary numbers due to the design of the pressure function. The results show that adding numerical diffusion to the ECPC scheme to create the ESPC scheme which did not change the solution to which the system converges.*

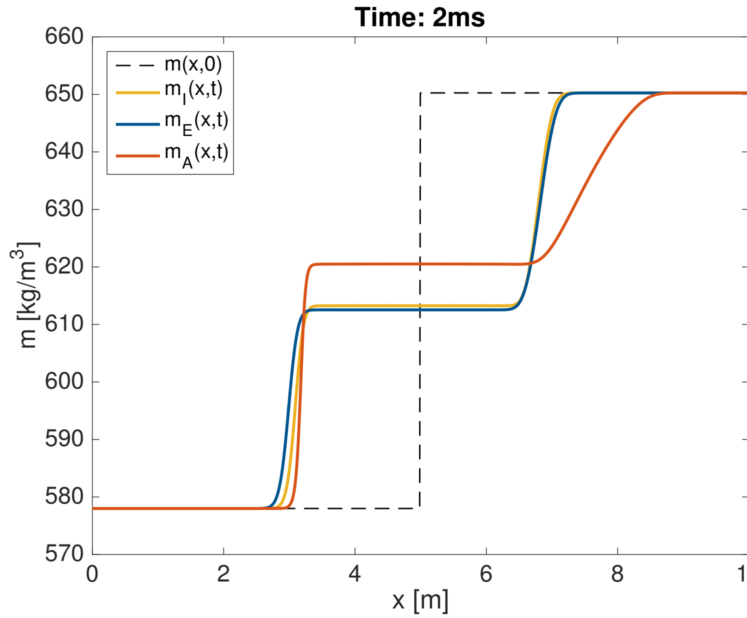

(a)

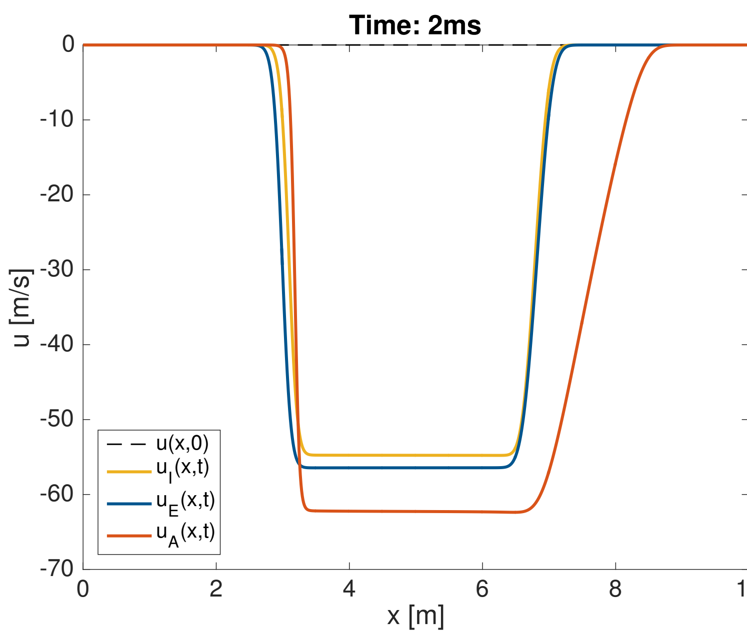

(b)

Figure 4.3: *Comparison between the three schemes defined in Chapter 3 for (a) liquid density m and (b) fluid velocity u. In the figure we can see that the Euler (E) and isentropic (I) systems yields similar result which is due to the similarity in their pressure expressions. The adiabatic (A) varies in both final amplitude but also in wave speed most notably for the expansion wave.*

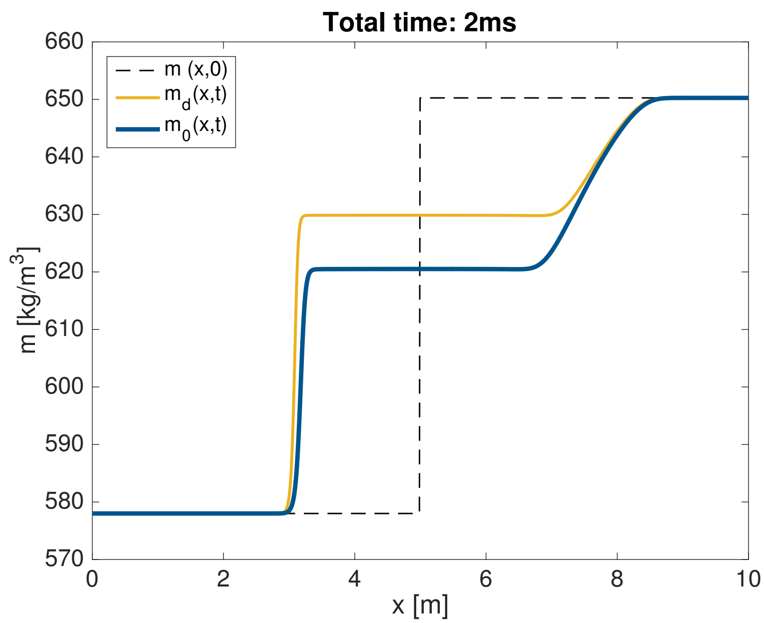

(a)

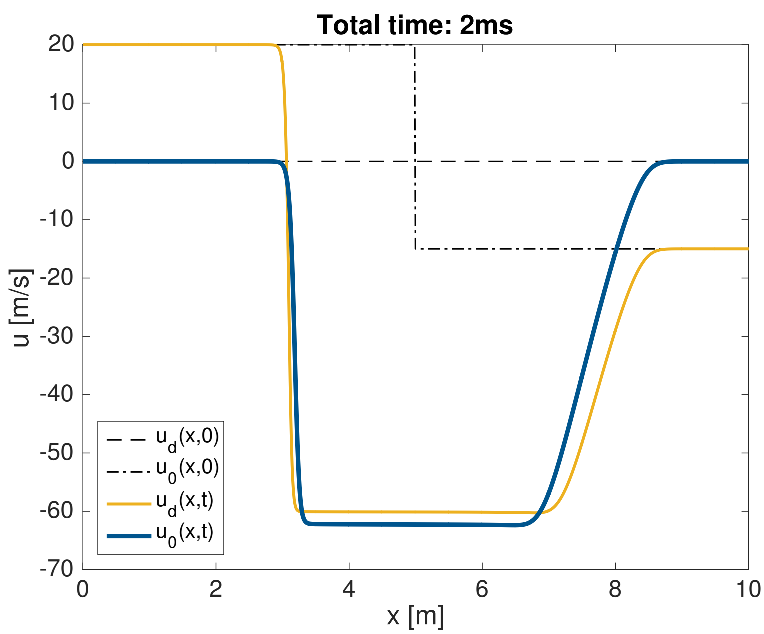

(b)

Figure 4.4: *The adiabatic system with different initial velocities (noted with index d) for (a) liquid density m and (b) fluid velocity u. From the results we can see that the final amplitude of the system depends on the initial velocity. In the figure we have that the final amplitude of the liquid density is increased as more fluid rushes in from both sides to mix in the middle.*

4.3 Two-sided Discontinuity

The other scenario studied in this thesis is a two-sided discontinuity caused by a sudden decrease in void fraction in a finite section of the pipe. Same as before we begin by comparing the ECPC and ESPC schemes and the results can be seen in Figure 4.5. From the results we see that we get similar results as the one-sided discontinuity case. The final amplitude are the same for both waves if we look at the mean of the oscillations for the ECPC scheme. The wave speed for the ESPC is slightly lower on the outer side of both waves. This behavior is similar to the left side of the previous case. The inner sides of the waves represent the right side of the previous scenario and again we have similar wave speeds for both schemes. Adding numerical diffusion slightly affects the wave speed and should be investigated further as future work. In the one-sided discontinuity case we had that the system stabilized at a final amplitude across the entire system. In this case the two waves form and simply travel in opposite directions without changing shape and will simply disappear once they travel out of the system. Once the waves have disappeared the system will be at rest at the value of the lower density value.

As for the one-sided discontinuity we compare the three schemes defined in Chapter 3 and we can see the results in Figure 4.6. As expected the results are as before with the Euler and isentropic systems yielding similar results while the adiabatic system has a steeper front shock wave and a wider expansion wave. Besides the difference in shape the adiabatic system also has a difference in amplitude but because m is a conserved variable the area of the waves are equal for all systems.

When the void fraction was lowered causing the discontinuity we can also assume that the velocity of the fluid was altered. In this example the velocity was lowered slightly and the results can be seen in Figure 4.7. As the fluid is generally moving to the right we can see that the waves are slightly different. Studying Figure 4.7a we see that the symmetry we previously had is broken with final amplitudes and wave speeds of the expansion waves differing slightly. In Figure 4.7b we get the same differences but also a general increase in amplitude due to a higher initial velocity.

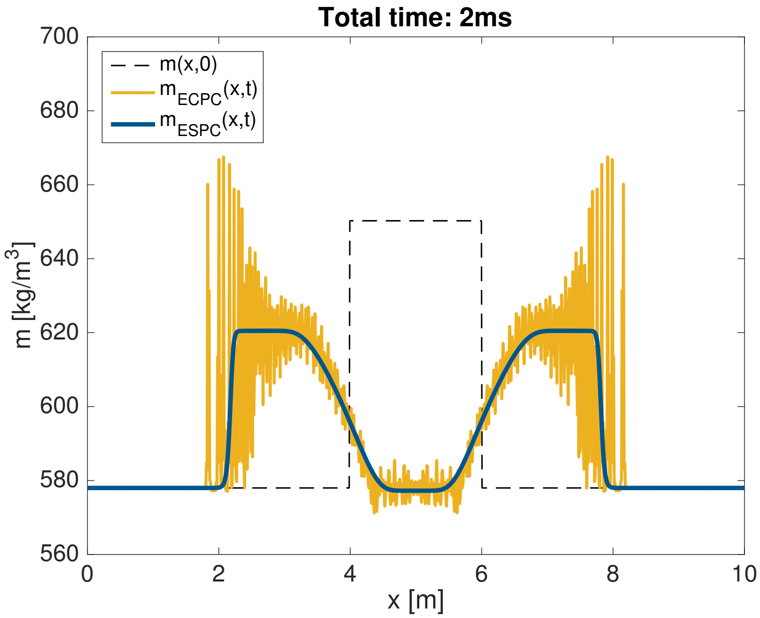

(a)

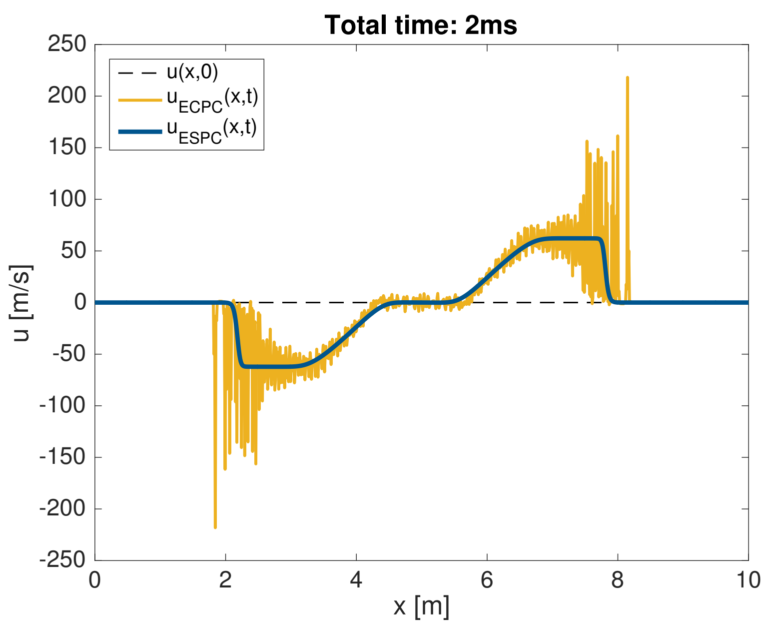

(b)

Figure 4.5: *Comparison between the ECPC and ESPC schemes for (a) liquid density m and (b) fluid velocity u. Both systems converge towards the same general solution but with the expected oscillations in the ECPC scheme. The oscillations will eventually cause the system to return imaginary numbers due to the design of the pressure function. The results show that adding numerical diffusion to the ECPC scheme to create the ESPC scheme did not change the solution to which the system converges. In this system the wave speeds that are still similar but the difference between the ESPC and ECPC schemes is more significant.*

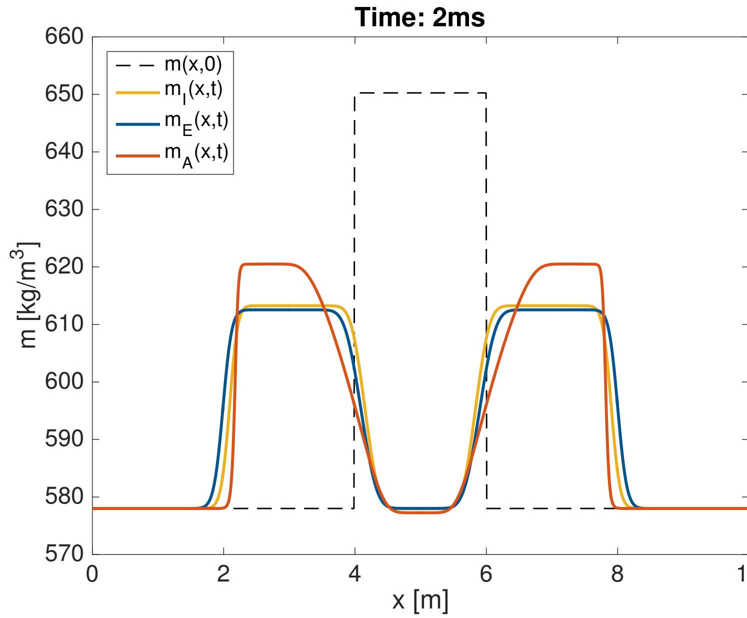

(a)

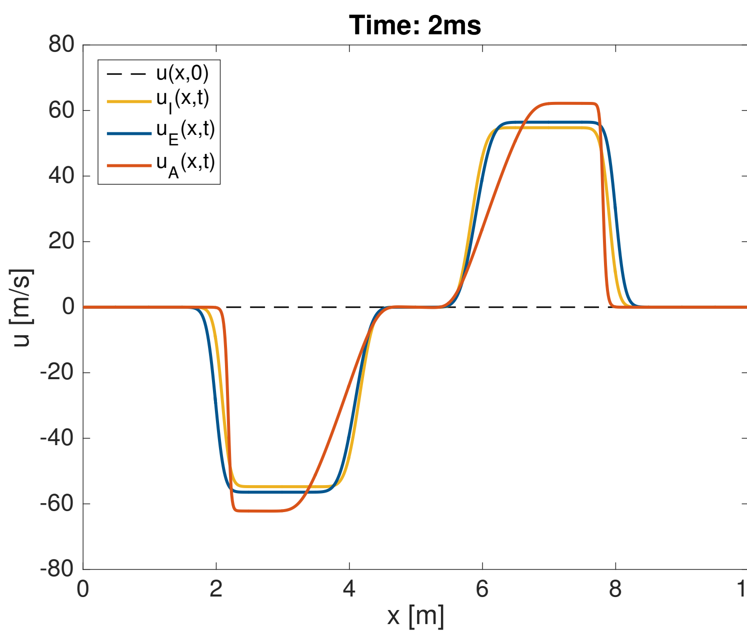

(b)

Figure 4.6: *Comparison between the three schemes defined in Chapter 3 for (a) liquid density m and (b) fluid velocity u. Similar to the one-sided discontinuity case we have that the Euler (E) and isentropic systems (I) yield similar results. The adiabatic (A) system yields a steeper shock wave in the front and wider expansion wave.*

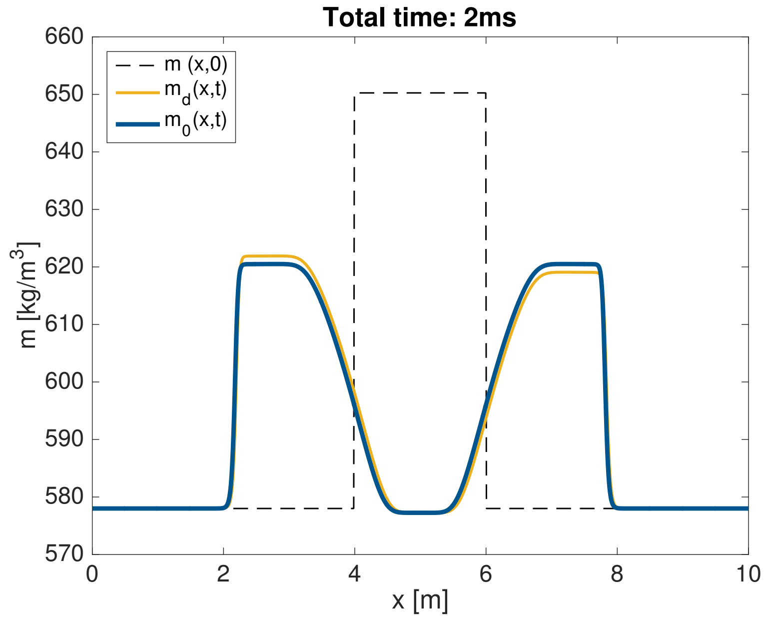

(a)

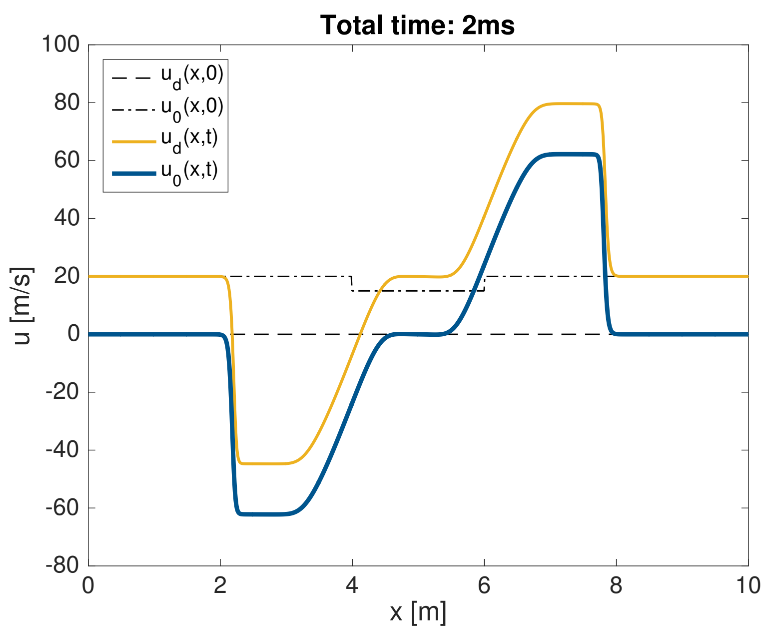

(b)

Figure 4.7: *The adiabatic system with different initial velocities (noted by the index d) for (a) liquid density m and (b) fluid velocity u. In this scenario we see that the velocity affects the system less than the one-sided discontinuity. The final amplitude is only slightly different and the wave speed of the expansion wave has been affected. Besides that we no longer have symmetry between the waves as fluid is collected in the left wave while being lower in the right wave.*

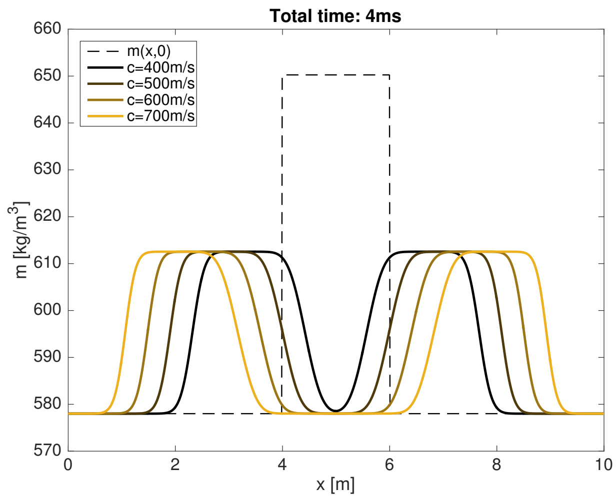

Figure 4.8: *Results for the Euler system for the case two-sided discontinuity with different values for the speed of sound. For the Euler system the constant is c^2 and the results show it does not affect the shape of the wave but only the wave speed.*

4.4 Reasons for Result Disparity

From the previous results we can see that the Euler (E) and isentropic (I) systems are quite similar in shape while the adiabatic (A) system varies in both shape and final amplitude. The Euler and isentropic system yield comparable results due to the similarity between their pressure expressions which is the only thing that differs between the three systems. Studying the pressure expressions

$$\begin{aligned} P_E &= c^2(m+n) \\ P_I &= K_I(m+n)^\gamma \\ P_A &= K_A\left(\frac{\rho_l n}{\rho_l - m}\right)^\gamma \end{aligned} \tag{4.1}$$

we see that all of them are of the form $P(m,n) = K\tilde{P}(m,n)$. The constant K is the largest factor for wave speed and does not affect the shape at all. We can see an example of this in Figure 4.8 where we see that changing the constant has no effect on the shape of the wave.

Since the constant does not affect the shape of the wave we instead look at the function $\tilde{P}(m,n)$ and how it is affected by a change in density. This can be seen in Figure 4.9. We can see that the adiabatic system is much more affected by changes in pressure and this is the reason for the spikier waves from this system.

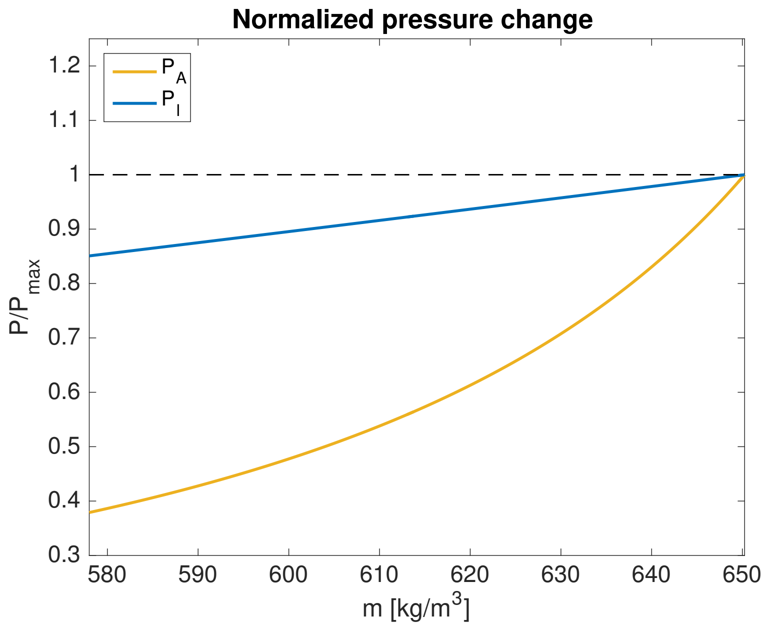

(a)

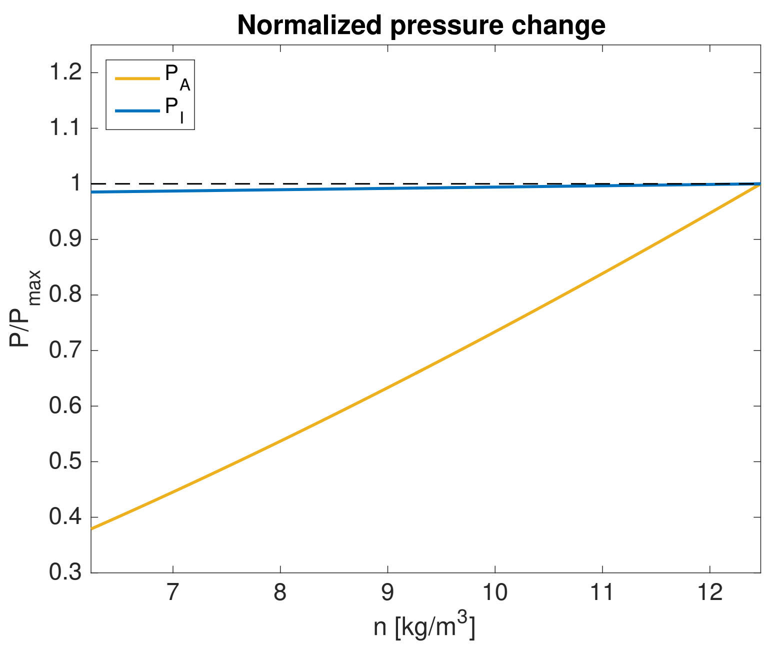

(b)

Figure 4.9: *Effect on the pressure due to change in a) liquid density m and b) vapour density n. We see that the adiabatic system (A) is greatly more affected by changes in density than the isentropic (I). Because the adiabatic system is much more sensitive to changes in density the resulting shock waves will be spikier.*

Chapter 5

Summary & Conculusions

In the nuclear power industry it is vital to understand the behaviour of the plant in order to conduct safe operations. As power plants are based on the steam power cycle we study the field of thermal hydraulics and the conservation equations associated with it. These conservation equations are differential in nature and cover the quantities mass, momentum, and also energy if the fluid is heated. To solve these equations we rely on computer codes such as TRACE which allows us to simulate both normal operations and accidents in the plant. TRACE uses first order accurate numerical solver based on the two-fluid model that uses flux limiter schemes to handle unphysical responses resulting from high order spatial discretization.

A system can be modelled using hyperbolic equations which relate to a set of conserved quantities. Studying the characteristics of non-linear hyperbolic systems can show possible shock formation as a result of discontinuities in the system. As the discontinuities makes the system non-differentiable we instead find weak solutions to the system and use additional conditions to find the physically correct solution. Systems such as these are hard to model and using simple numerical methods will result in oscillations and diffusion. Instead we use entropy and path conditions to construct numerical schemes commonly referred to as ESPC. To construct our model we started with a basic two-fluid model and through some approximations we were able to create a hyperbolic system of two-phase equations. From this we had a choice in how to model the pressure in the system and in this thesis we studied three models. The first was based on the isothermal Euler equations, the second was based on being an isentropic polytropic gas, and the last based on the adiabatic process. The first two are based on one-phase systems that were previously studied while the last system is a pure two-phase system.

The systems are tested on two scenarios; the first one being a single discontinuity made to model flow reversal and the second scenario model decreased void in a finite volume resulting in a two-sided discontinuity. The first test for both scenarios is to compare the differences between entropy conservative and stable systems. This shows how adding the diffusion operator affects the oscillations in the system but also to confirm that the system still converges to a physical solution. In the next test we compare the three systems and we see similar results for the Euler and isentropic systems which was expected while the adiabatic system differs slightly. Compared to the Euler and isentropic systems the adiabatic system is a lot more sensitive to small changes in density which is the cause for the differing results. The last test shows how the adiabatic system is affected by changing the initial velocities. For the scenario of the one-sided discontinuity the two fluids crash into each other resulting in a higher final amplitude. For the two-sided discontinuity scenario the symmetry we previously had has been broken but overall the final amplitude is less affected in this scenario.

In this thesis we have constructed three ESPC schemes for a two-phase systems with pressure based on the isothermal Euler equations, isentropic process, and adiabatic process. The first two systems are based on previously studied one-phase systems and was used for comparion to the adiabatic system which purely two-phase and has not been studied before. The results show that adding the diffusion operator affects the wave speed which previous studies has confirmed. This might mean that the system is no longer converging towards a physical solution and should be studied further. Comparing the results from the adiabatic system with the other ones also shows a disparity in results which is partly due to how sensitive the pressure in the adiabatic system is to changes in density. Due to the lack of two-phase numerical schemes that do not rely on unphysical methods such as flux limiter further work should be done in this field.

Bibliography

[1] Nuclear Regulatory Commision. Computer codes. https://www.nrc.gov/about-nrc/regulatory/research/safetycodes.html. Accessed: 2017-04-27.

[2] Strålsäkerhetsmyndigheten. Implementering och underhåll av termohydrauliska datorprogram under 2011. https://www.stralsakerhetsmyndigheten.se/Global/Forskning/Beslutade%202011/Kärnkraftssäkerhet/SSM2011-1574%20Implementering%20och%20underhåll%20av%20termohydrauliska%20datorprogram%20under%202011.pdf. Accessed: 2017-05-28, Swedish.

[3] E. Tadmor. The numerical viscosity of entropy stable schemes for systems of conservation laws. I. *Mathematics of Computation*, 49:91–103, 1987.

[4] M.J. Castro, U. S. Fjordholm, S. Mishra and C. Parés. Entropy conservative and entropy stable schemes for non-conservative hyperbolic systems. *ESAIM: Mathematical Modelling and Numerical Analysis*, 2011.

[5] R. J. LeVeque. *Numerical Methods for Conservation Laws.* Birkhäuser, 1999.

[6] M. J. Castro, M. L. Muños, C. Parés. Physical viscosity numerical methods for non-conservative hyperbolic systems. http://www.mat.ucm.es/~homenajeJIDiaz60/advertisement&abstract/collectedabstract/Pares_AbstractJIDiaz60.pdf. Accessed: 2017-05-21.

[7] R. Abgrall, S. Karni. A comment on the computation of non-conservative products. *Journal of Computational Physics*, 229:2759–2763, 2010.

[8] E. Tadmor. Entropy stability theory for difference approximations of nonlinear conservation laws and related time-dependent problems. *Acta Numerica*, 12, 05 2003.

[9] S.T. Munkefjord, S. Evje and T. Flåtten. A musta scheme for a non-conservative two-fluid model. *SAIM: Journal on Scientific Computing*, 31, 2011.

[10] U. S. Fjordholm and S. Mishra. Accurate numerical discretizations of non-conservative hyperbolic systems. *ESAIM: Mathematical Modelling and Numerical Analysis*, 46:187–206, 2012.

[11] S. Evje, K. Karlsen. Global existence of weak solutions for a viscous two-phase model. *Journal of Differential Equations*, 245, 2008.